Protostars: Forges of Cosmic Rays?

Marco Padovani

INAF-Osservatorio Astrofisico di Arcetri - Firenze

Alexandre Marcowith – Patrick Hennebelle – Katia Ferrière

Daniele Galli – Al Glassgold – Alexei Ivlev – Paola Caselli

Padovani, M., Hennebelle, P., Marcowith, A. & Ferrière, K. (2015) A&A 582, L13

Padovani, M., Marcowith, A., Hennebelle, P. & Ferrière, K. (2016) A&A 590, A8

Padovani, M., Marcowith, A., Hennebelle, P. & Ferrière, K. (2017) PPCF, 59, 014002

Cosmic rays and interstellar medium in one slide

CRs

astrochemistry

see e.g. Caselli & Ceccarelli (2012) for a recent review

collapse timescale

Nakano+ (2002)
Padovani+ (2013,2014)

gas temperature

Glassgold & Langer (1973)
Cravens & Dalgarno (1978)
Dalgarno+ (1999)
Glassgold+ (2012)
Galli & Padovani (2015)

dust grain charge

Prasad & Tarafdar (1983)
Cecchi-Pestellini & Aiello (1992)
Shen+ (2004)
Ivlev+ (2015)

(production of light elements, γ-ray emission through π^0 decay...)

Cosmic rays and ASTROCHEMISTRY

see Caselli & Ceccarelli (2012) for a recent review

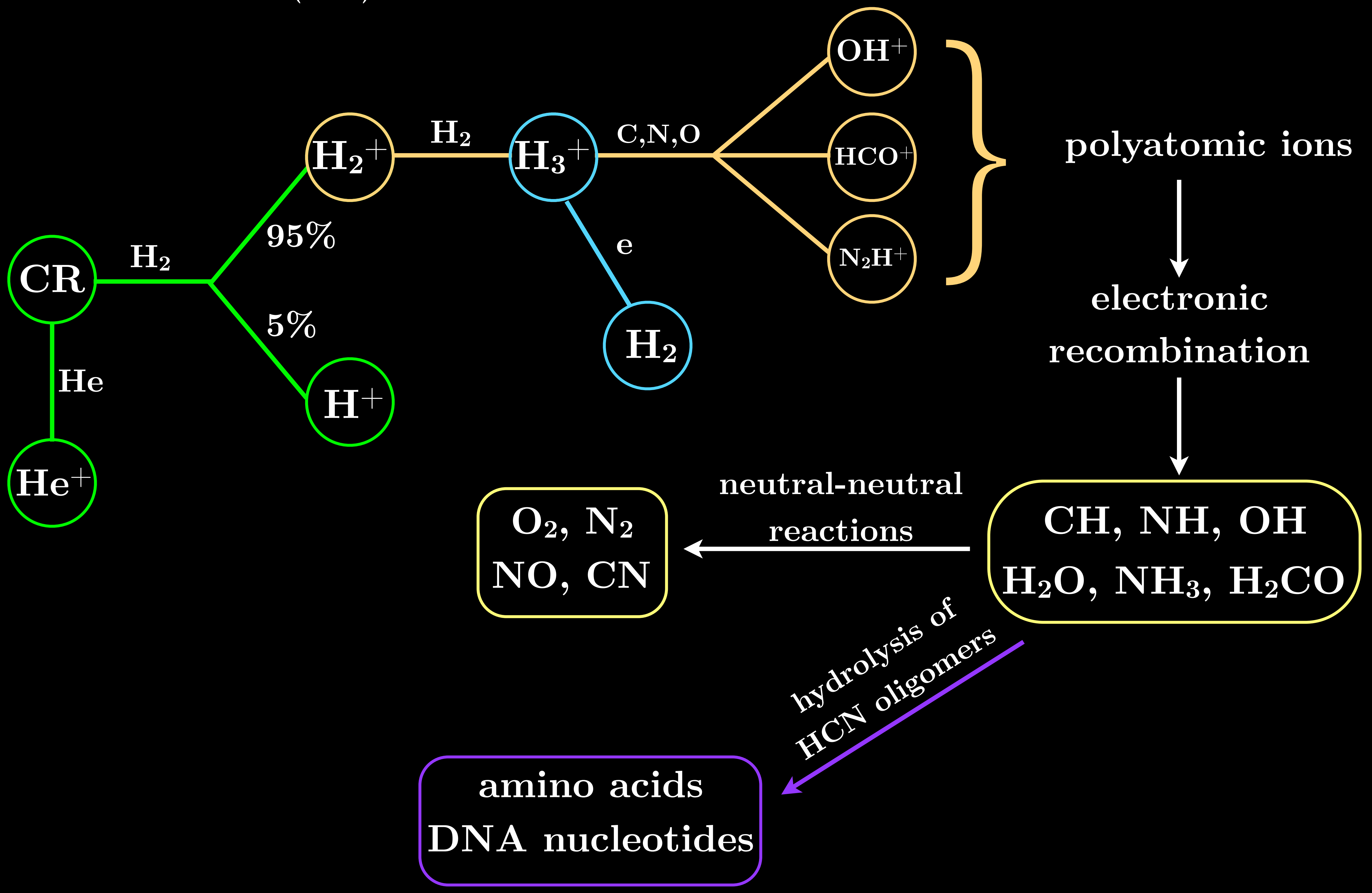

Cosmic-ray ionisation rate

(number of ionisation per second)

ζ [s^{-1}] → *key-brick parameter:*

— chemical models (interpretation of observed abundances);

— non-ideal MHD simulations (study of the collapse of a molecular cloud core and the formation of a protostellar disc);

$$\zeta = 4\pi \int j(E)\sigma(E)\mathrm{d}E$$

Cosmic-ray ionisation rate

CR protons

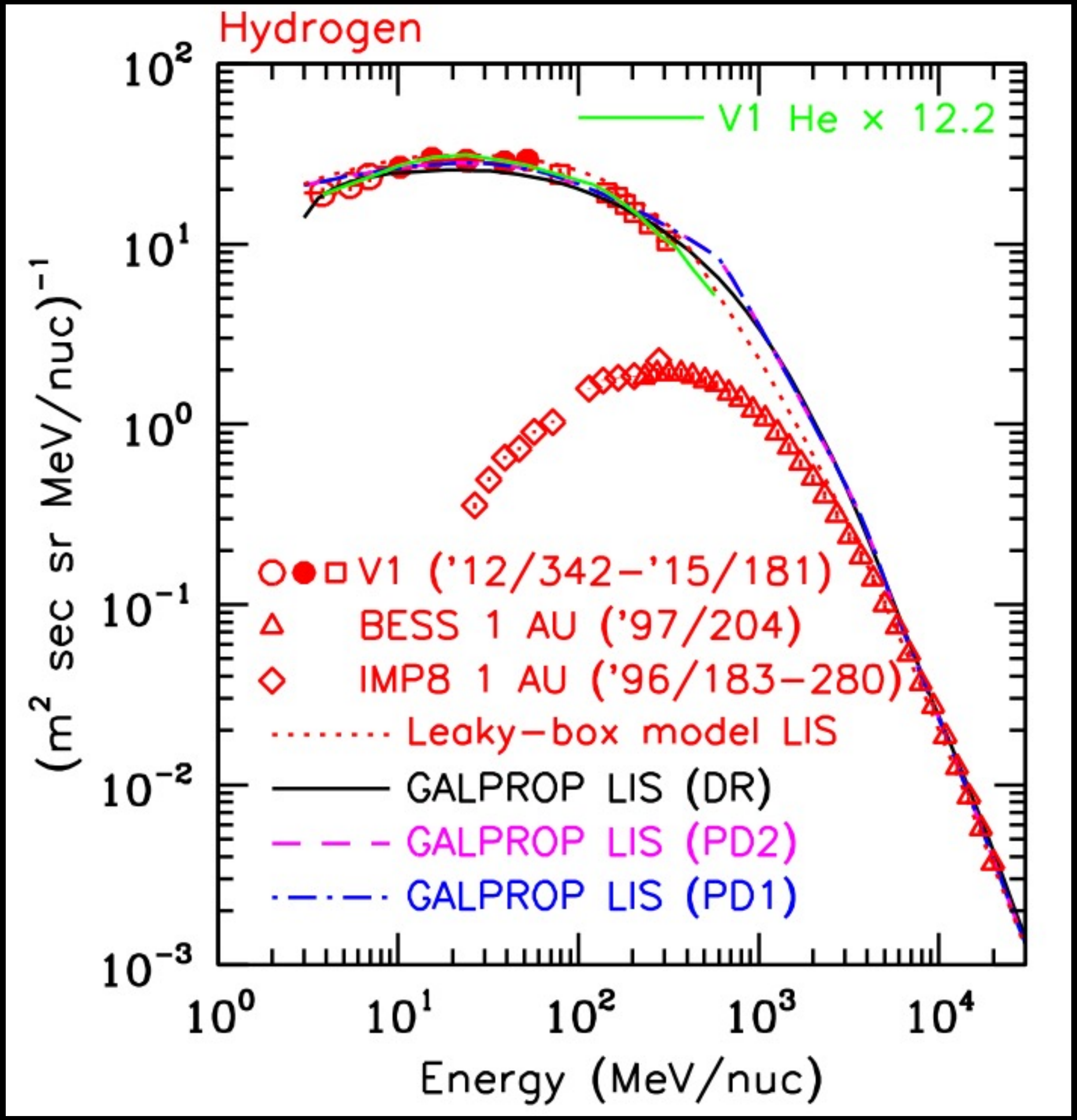

Cummings+ (2016)

CR electrons

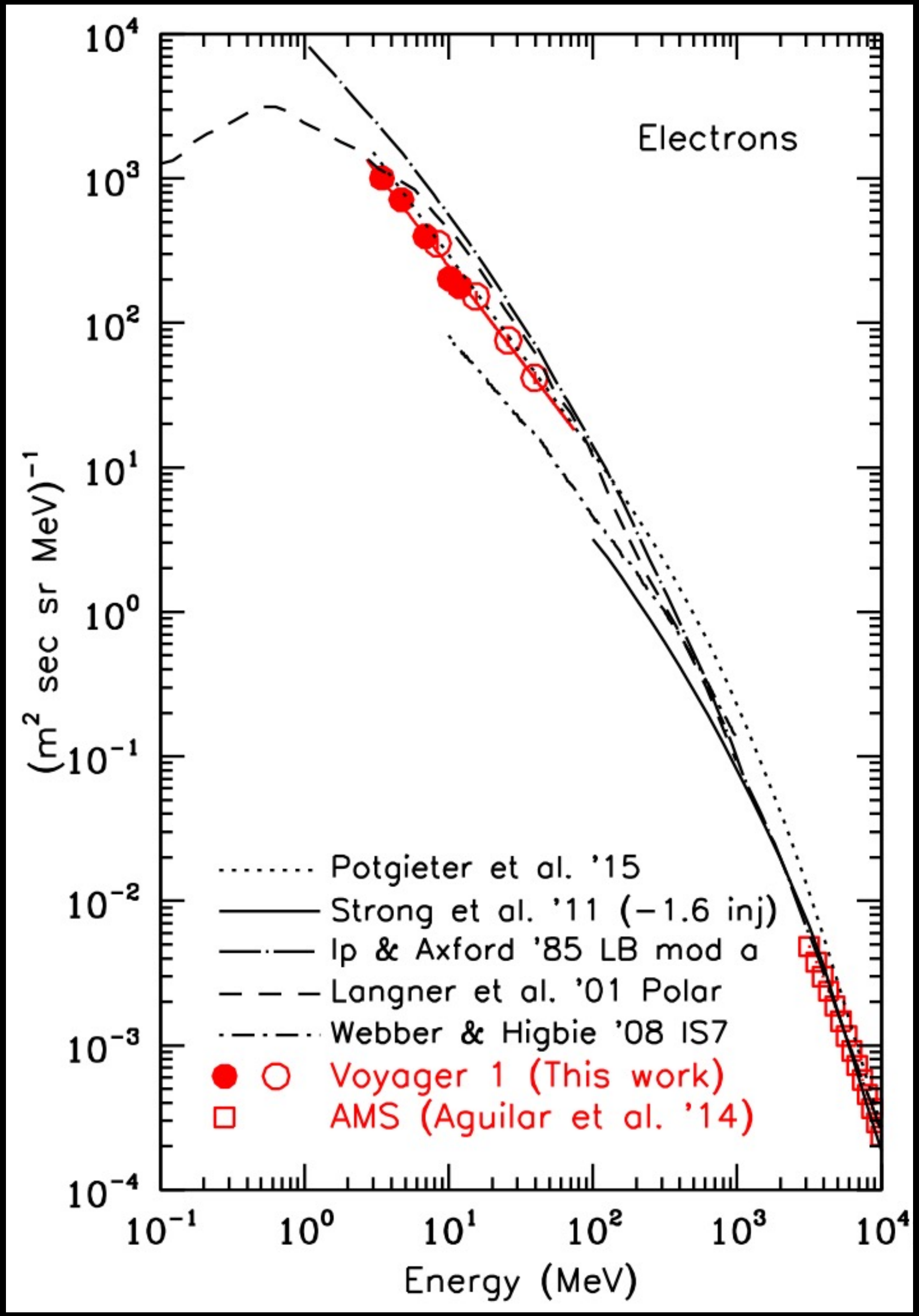

Cummings+ (2016)

Magnetic field:

- in the ISM (black lines);
- from the Sun (white lines).

Next expected signature:
variation in the magnetic field direction

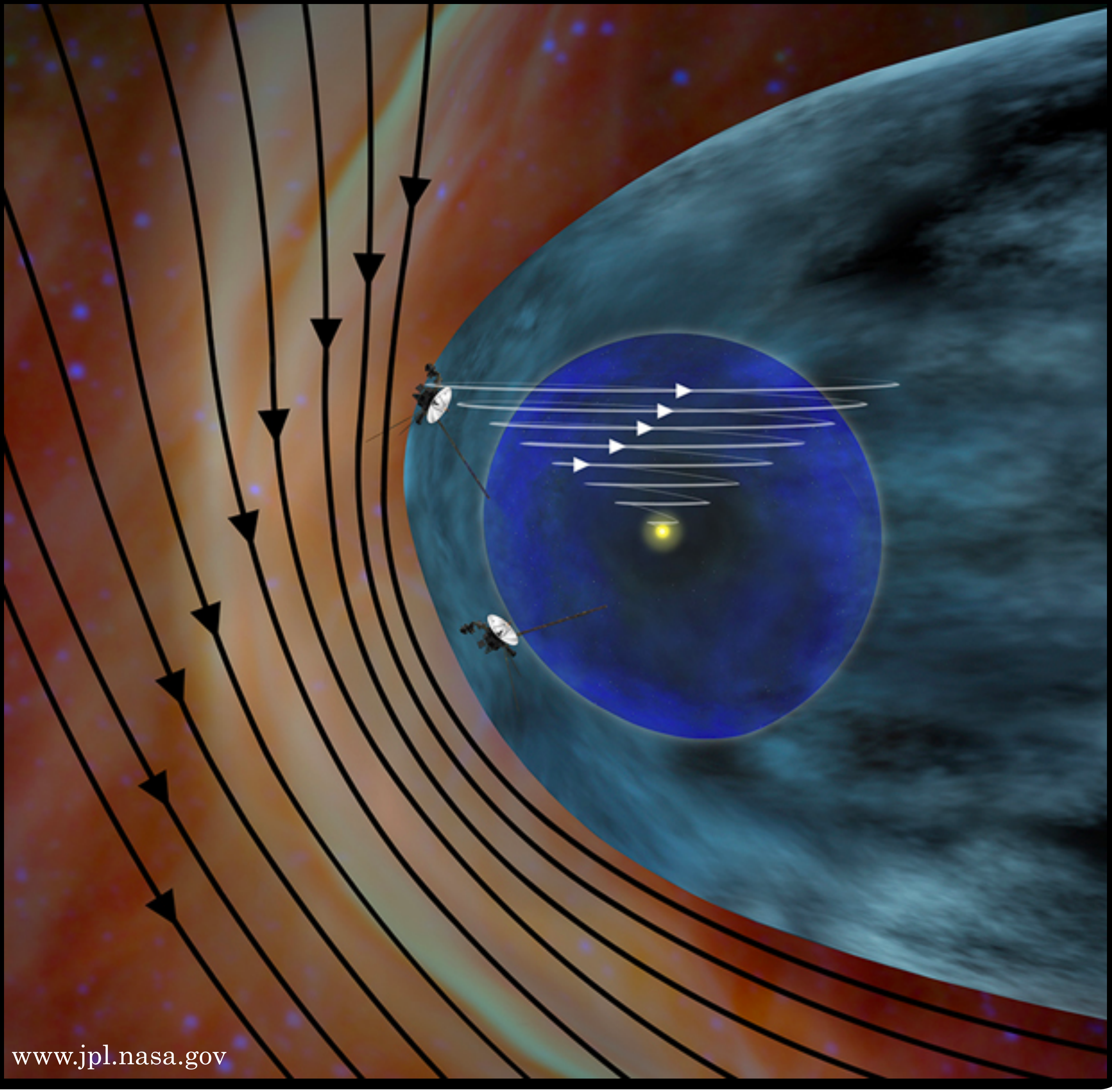

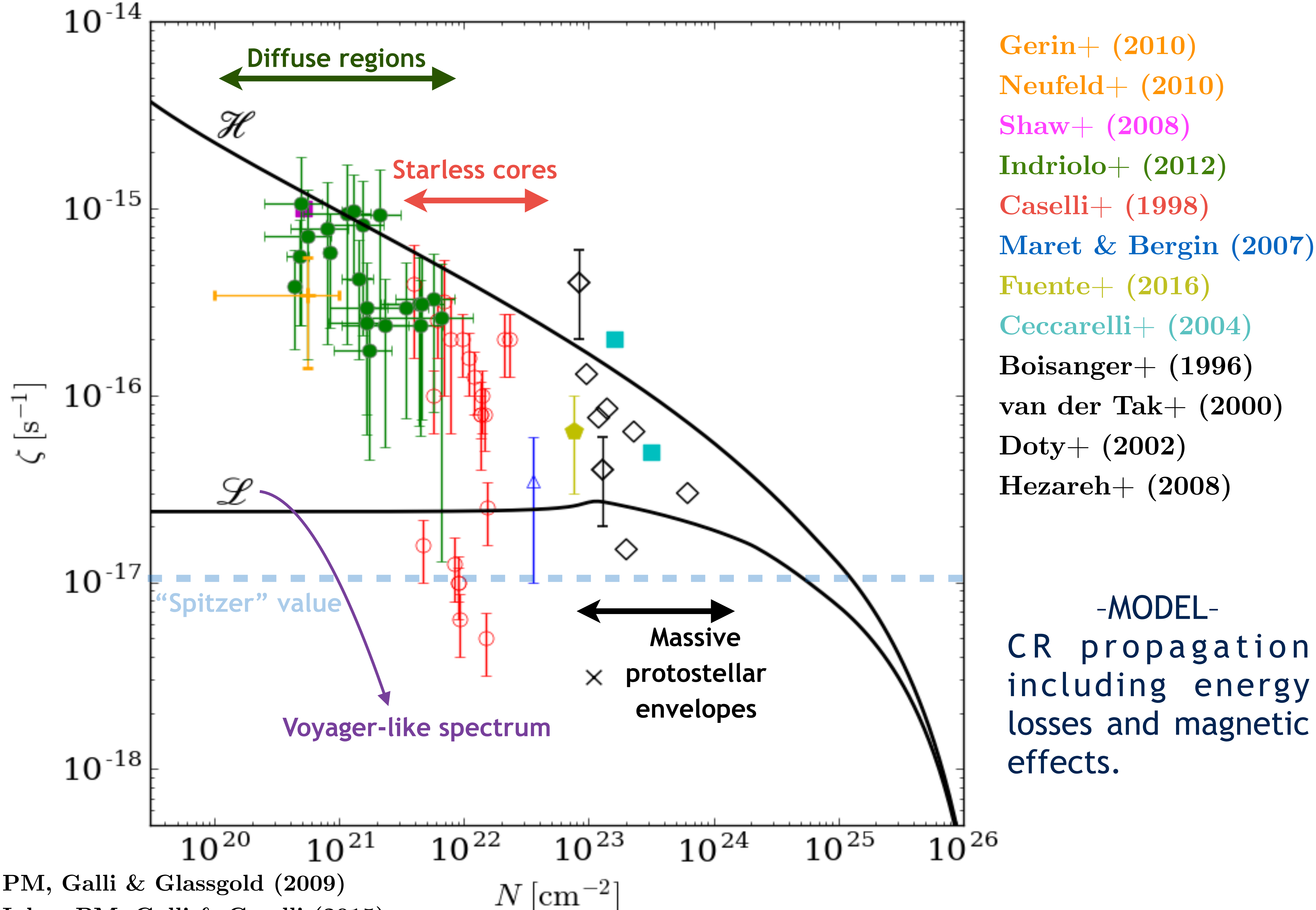

-MODEL-

CR propagation including energy losses and magnetic effects.

PM, Galli & Glassgold (2009)

Ivlev, PM, Galli & Caselli (2015)

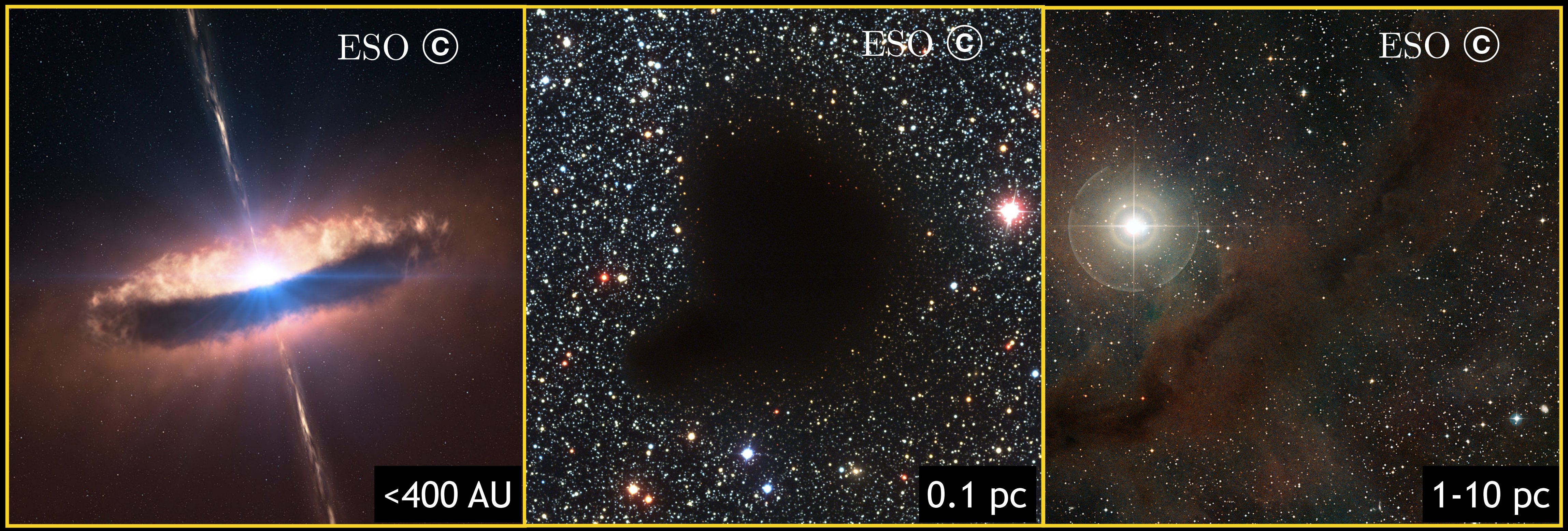
ESO ©
<400 AU
ESO ©
0.1 pc
ESO ©
1-10 pc

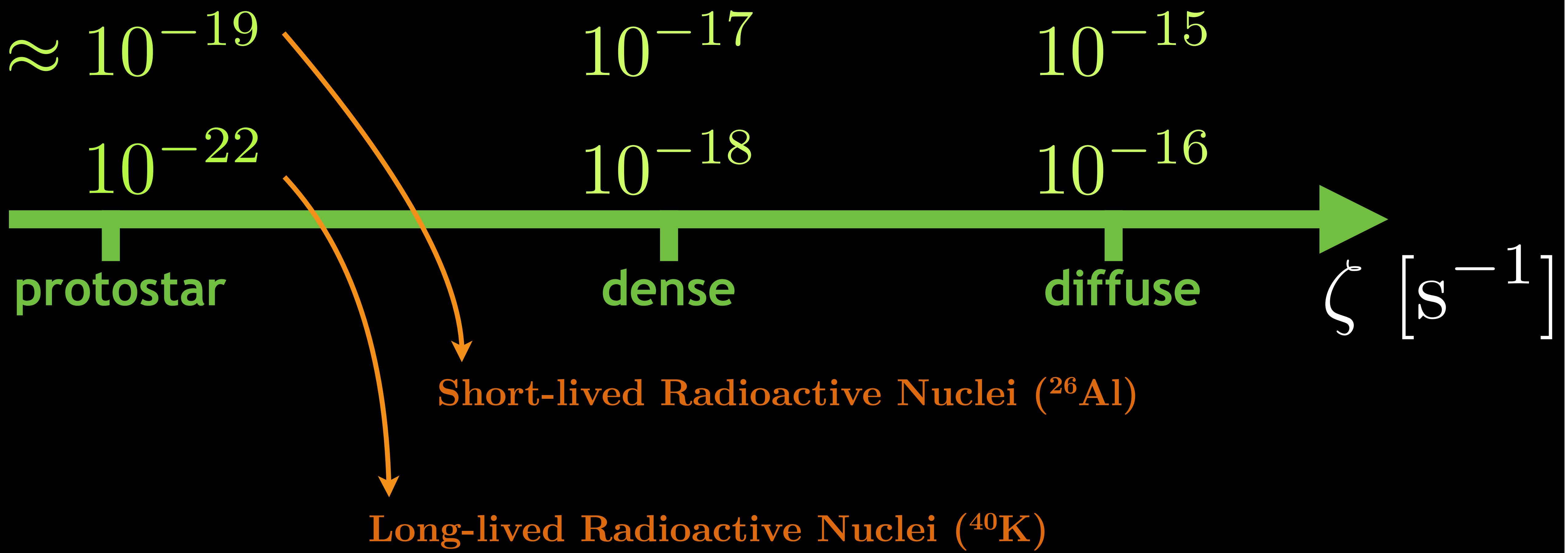
$\approx 10^{-19}$
10^{-22}
10^{-17}
10^{-18}
10^{-15}
10^{-16}
protostar
dense
diffuse
$\zeta\ [\mathrm{s}^{-1}]$
Short-lived Radioactive Nuclei (^{26}Al)
Long-lived Radioactive Nuclei (^{40}K)

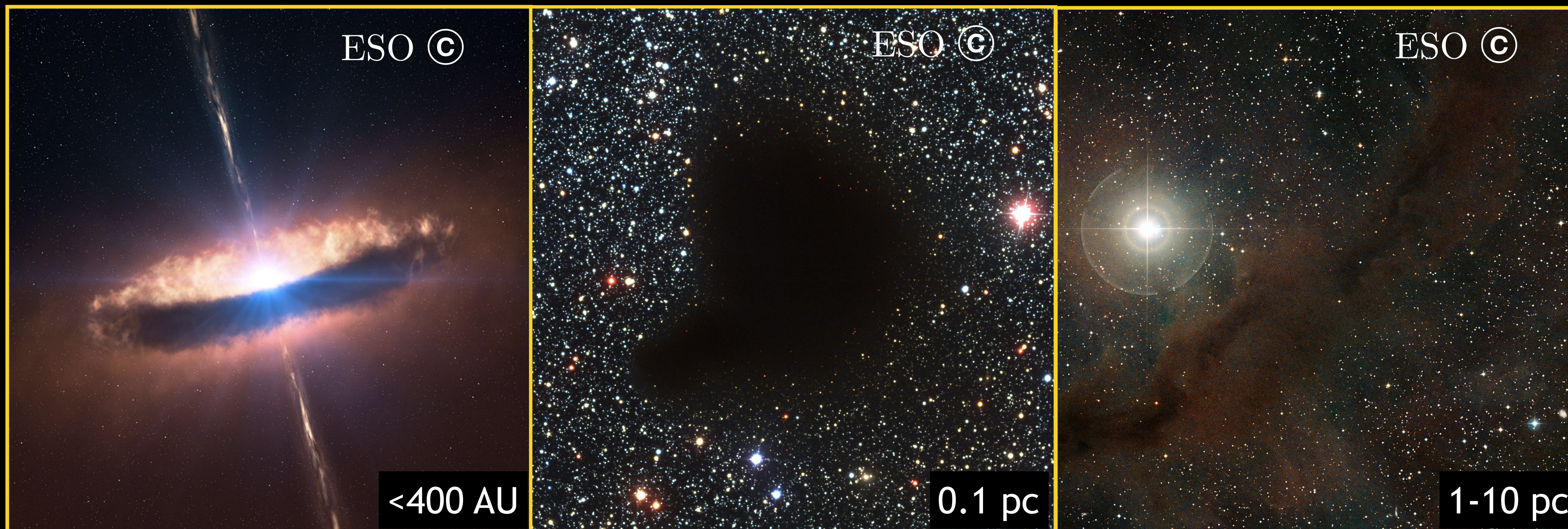

$\approx 10^{-19}$ | 10^{-17} | 10^{-15}

10^{-22} | 10^{-18} | 10^{-16}

protostar — dense — diffuse → $\zeta\ [\mathrm{s}^{-1}]$

- $\zeta \sim 3\times10^{-16}\ \mathrm{s}^{-1}$ in L1157-B1 (Podio+ 2014)
- $\zeta \sim 4\times10^{-14}\ \mathrm{s}^{-1}$ and $8\times10^{-12}\ \mathrm{s}^{-1}$ in OMC-2 FIR 4 (Ceccarelli+ 2014)
- $S_\nu \propto \nu^{-0.89\pm0.07}$ in the bow shock of DG Tau (Ainsworth+ 2014)

CR propagation in 3D simulations of collapsing rotating core

Intermediate magnetisation λ=5
Perpendicular rotator (**J**,**B**)=π/2

Field lines in the inner 600 AU

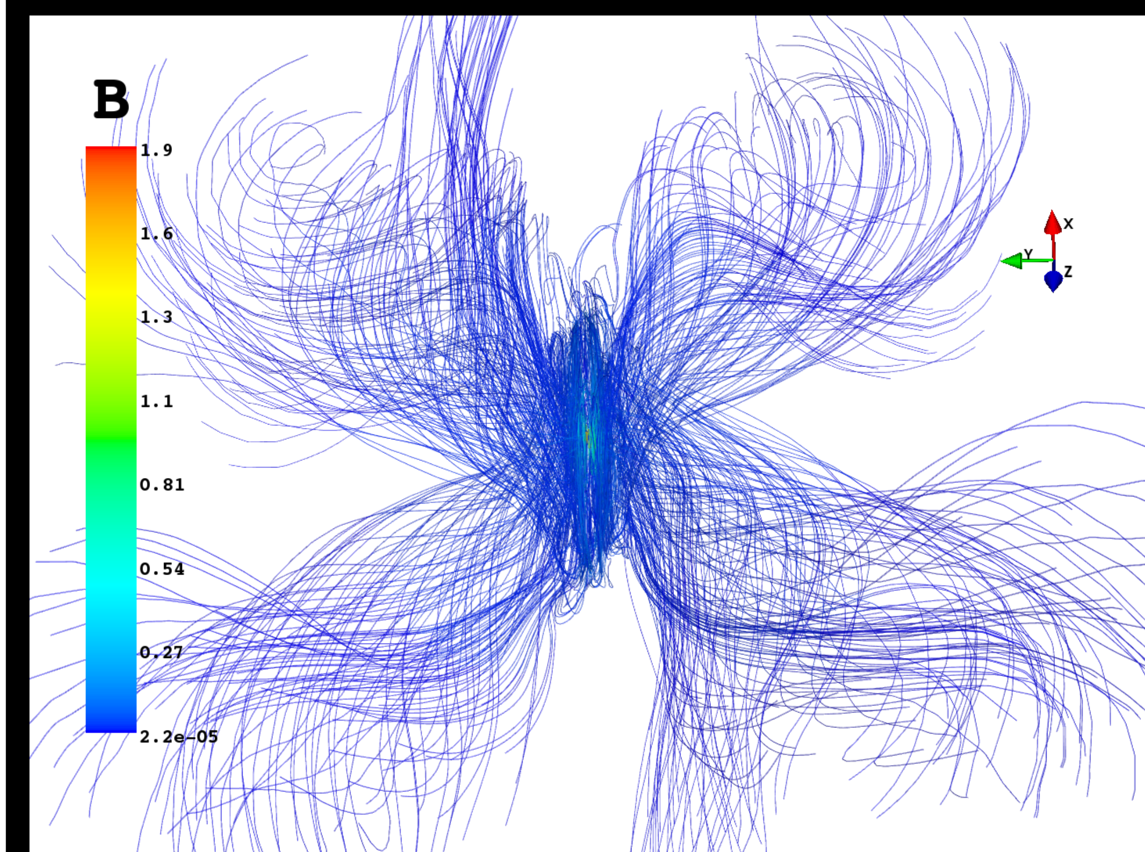

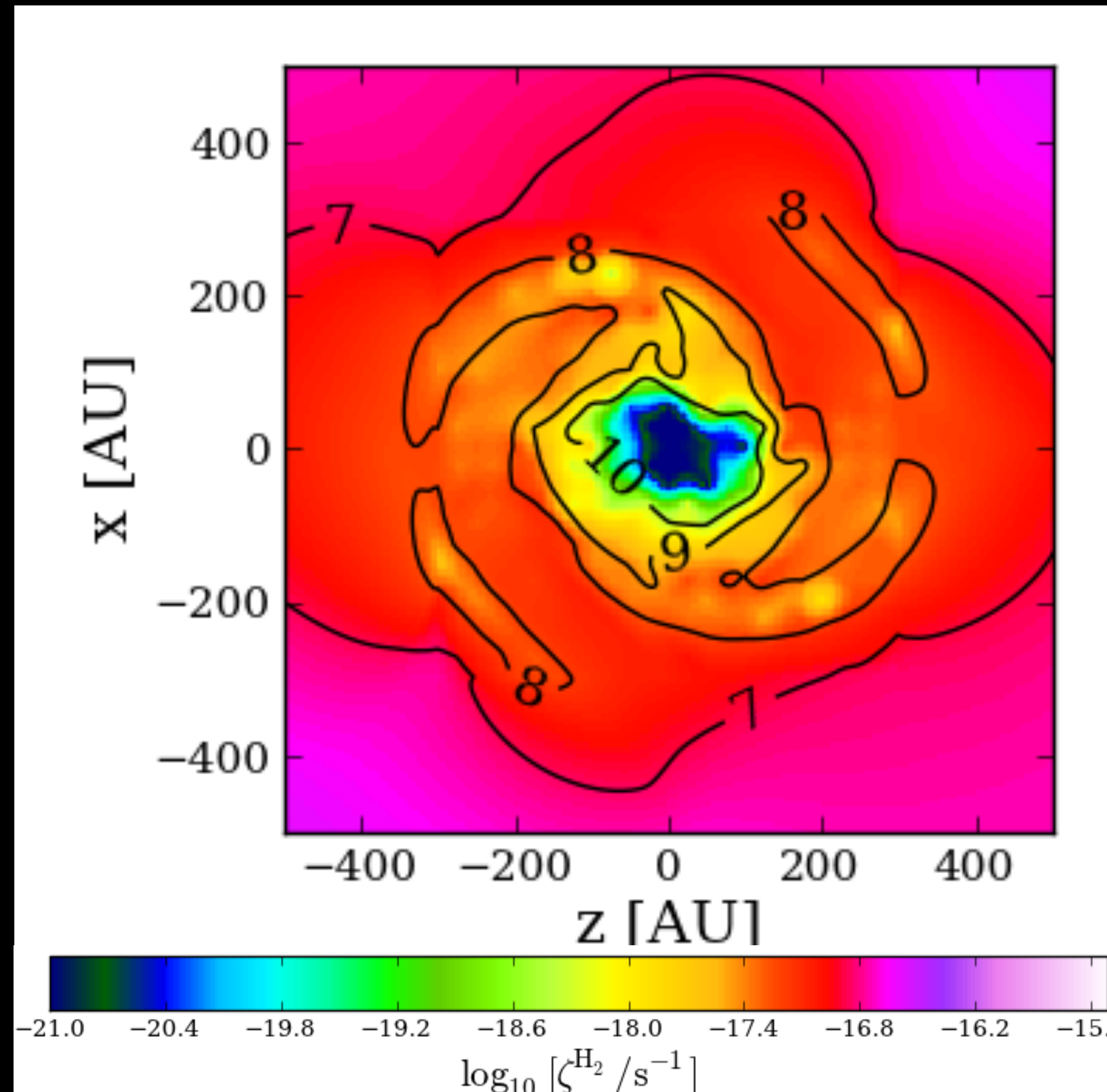

PM, Hennebelle & Galli (2013)

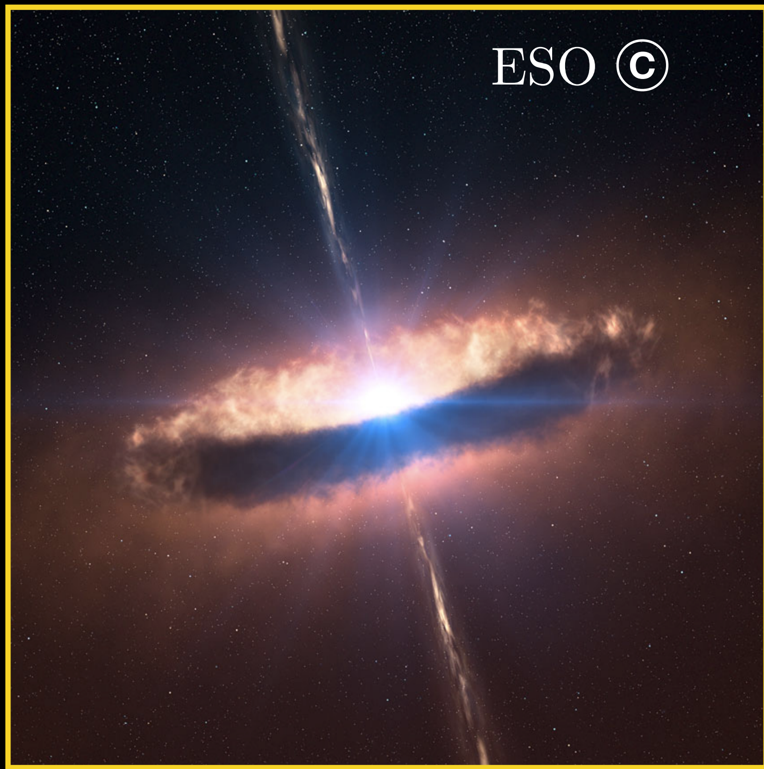

$\approx 10^{-19}$

10^{-22}

protostar

What are the possible sources of energetic particles?

- ζ~3×10^{-16} s^{-1} in L1157-B1 (Podio+ 2014)
- ζ~4×10^{-14} s^{-1} and 8×10^{-12} s^{-1} in OMC-2 FIR 4 (Ceccarelli+ 2014)
- $S_\nu \propto \nu^{-0.89\pm0.07}$ in the bow shock of DG Tau (Ainsworth+ 2014)

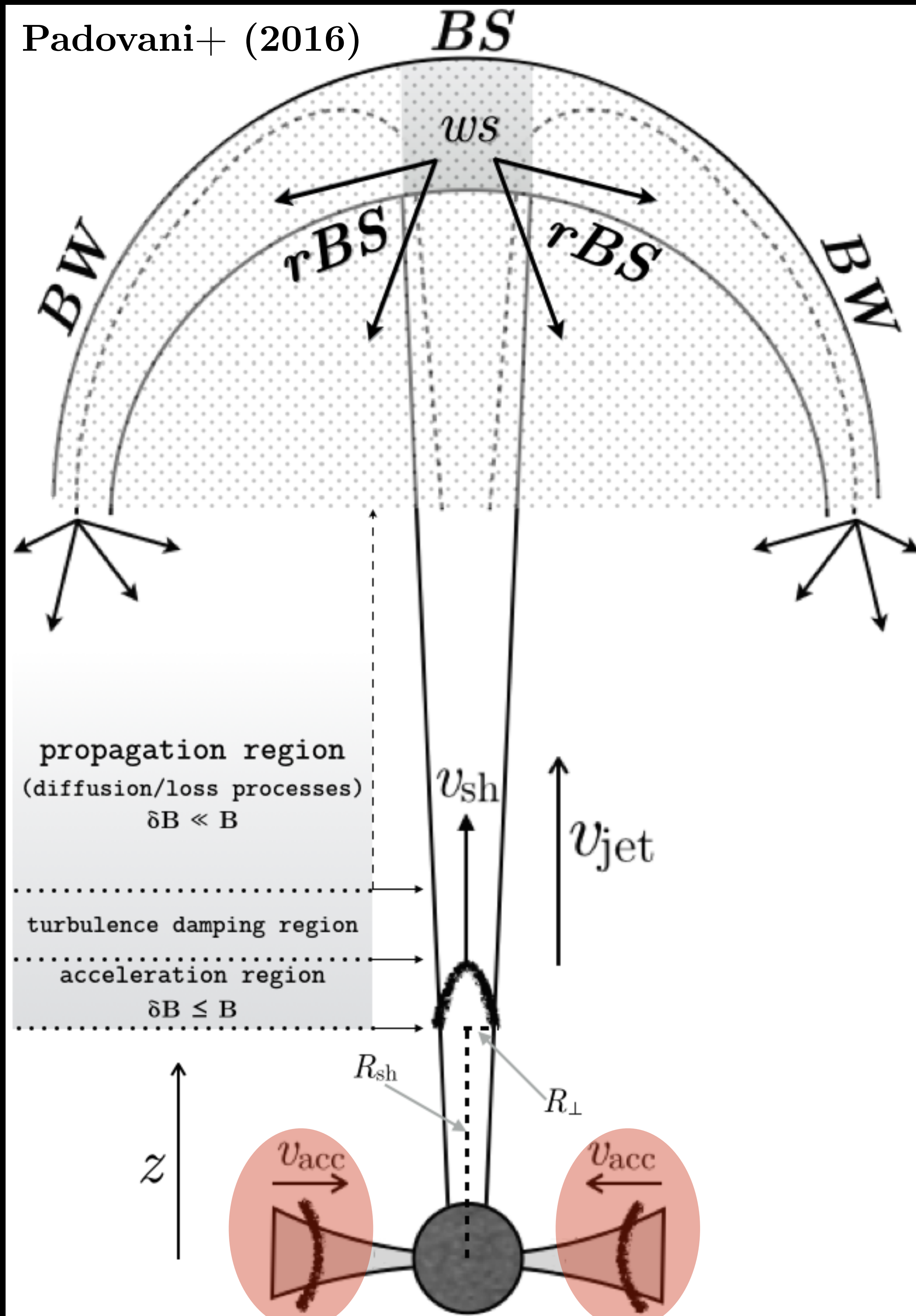

Acceleration sites

(1) accretion flows;

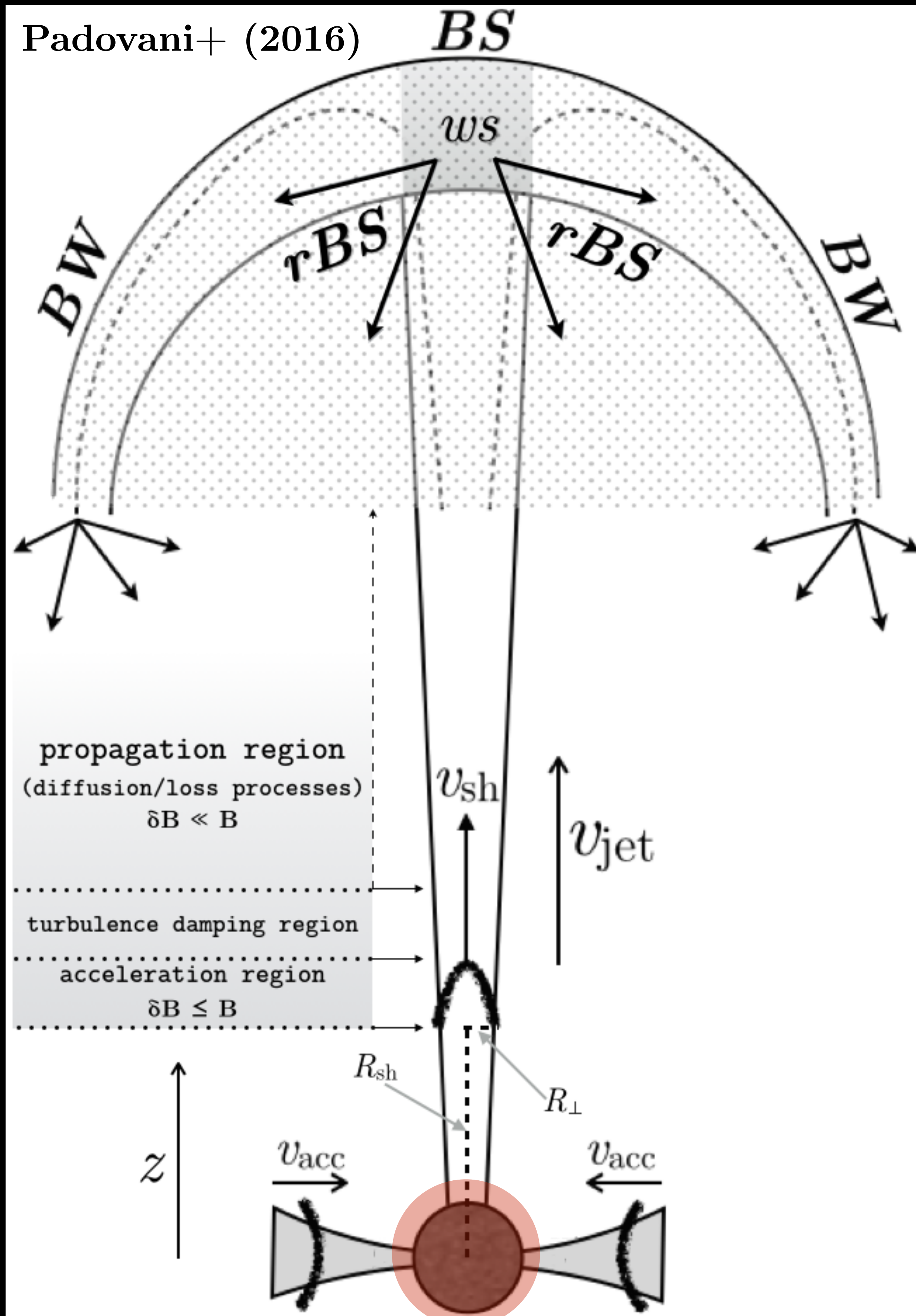

Acceleration sites

(1) accretion flows;

(2) protostellar surface;

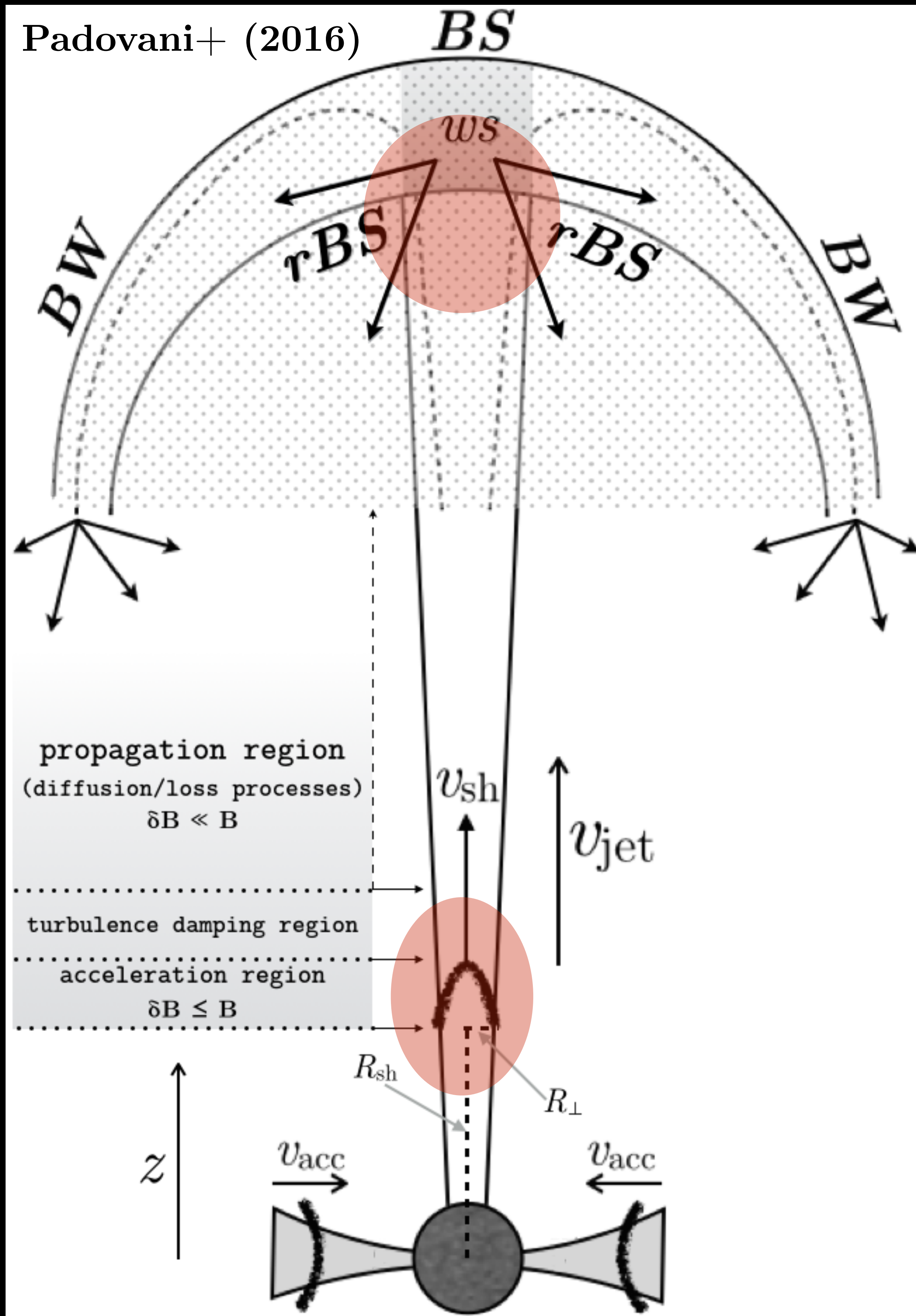

Acceleration sites

(1) accretion flows;

(2) protostellar surface;

(3) jet shock;

Padovani+ (2016)

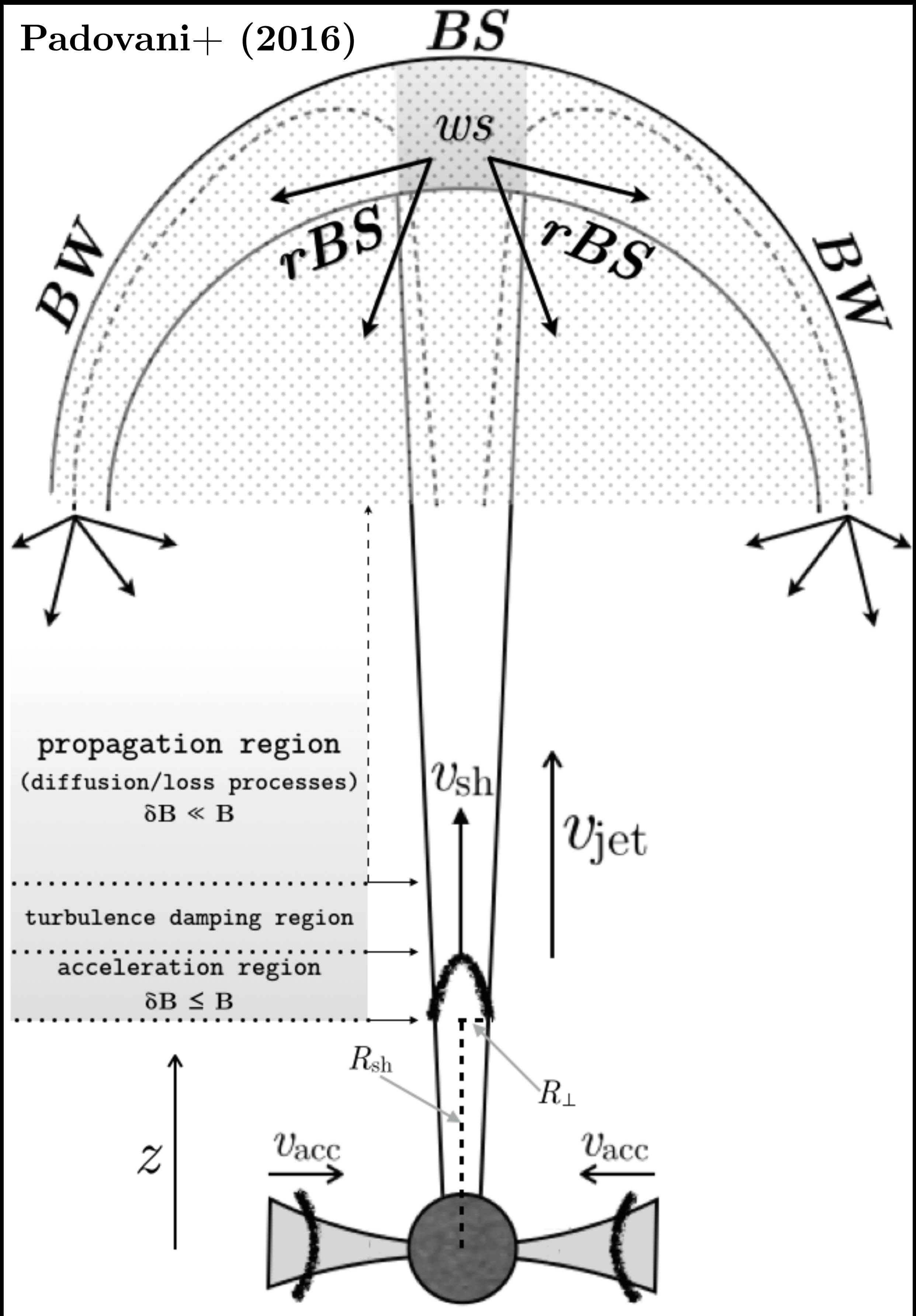

Acceleration sites

(1) accretion flows;
(2) protostellar surface;
(3) jet shock;

Diffusive Shock Acceleration (DSA) or First-order Fermi acceleration

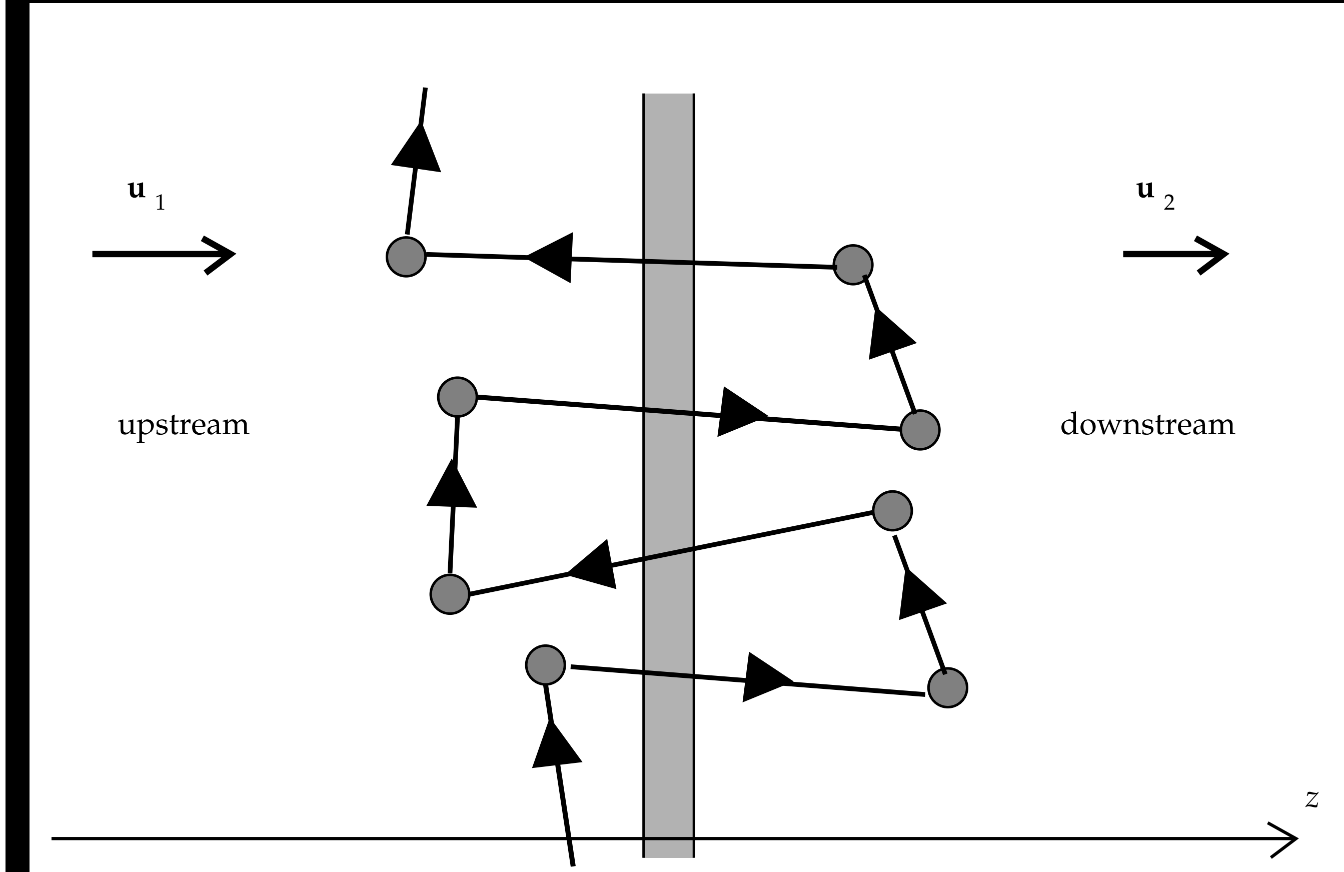

Melrose (2009)

Conditions to be fulfilled

Condition on flow velocity: **supersonic** and **super-Alfvénic**.

(1) **acceleration time shorter** than **collisional loss time**;

(2) **acceleration time shorter** than **dynamical time**;

(3) **shock geometry**: particles have to be accelerated before they start to escape by diffusion processes.

Presence of an ***incomplete ionised medium***: neutrals can decrease the effectiveness of the DSA mechanism damping the particle's self-generated Alfvén waves that are responsible of the particle scattering back and forth the shock (Drury+ 1996).

$$t_{\rm acc} = \min(t_{\rm loss}, t_{\rm esc,u}, t_{\rm esc,d}, t_{\rm dyn}) \to E_{\rm max}$$

Parameters needed for the model

site*	U [km s^{-1}]	T [K]	n_H [cm^{-3}]	x	B [G]
$\mathscr{E}$	$1-10$	$50-100$	10^7-10^8	$\lesssim 10^{-6}$	$10^{-3}-10^{-1}$
$\mathscr{J}$	$40-160$	10^4-10^6	10^3-10^7	$0.01-0.9$	$5\times10^{-5}-10^{-3}$
$\mathscr{P}$	260	9.4×10^5	1.9×10^{12}	$0.01-0.9$	$1-10^3$

*$\mathcal{E}$ = envelope $\mathcal{J}$ = jet $\mathcal{P}$ = protostellar surface

Refs: U_{sh} (Raga+ 2002,2011; Hartigan & Morse 2007; Agra-Amboage+ 2011);
T (Frank+ 2014);
n_H (Lefloch+ 2012; Gómez-Ruiz+ 2012);
x (Nisini+ 2005; Podio+ 2006; Antoniucci+ 2008; Garcia López+ 2008; Dionatos+ 2010; Frank+ 2014; Maurri+ 2014);
B (Tesileanu+ 2009, 2012)
For protostellar surface shock, parameters from Masunaga & Inutsuka (2000)

- DSA works *only* for protons (electrons lose energy too fast, $E^{max}(e)$<300 MeV);
- DSA is effective *only* in jet and protostellar surface shocks (in accretion flows, x and U_{sh} are too small, quenching the particle acceleration; B is as large as to produce a sub-Alfvénic shock).

Maximum Energy

$$t_{\rm acc} = \min(t_{\rm loss}, t_{\rm esc,u}, t_{\rm esc,d}, t_{\rm dyn}) \rightarrow E_{\rm max}$$

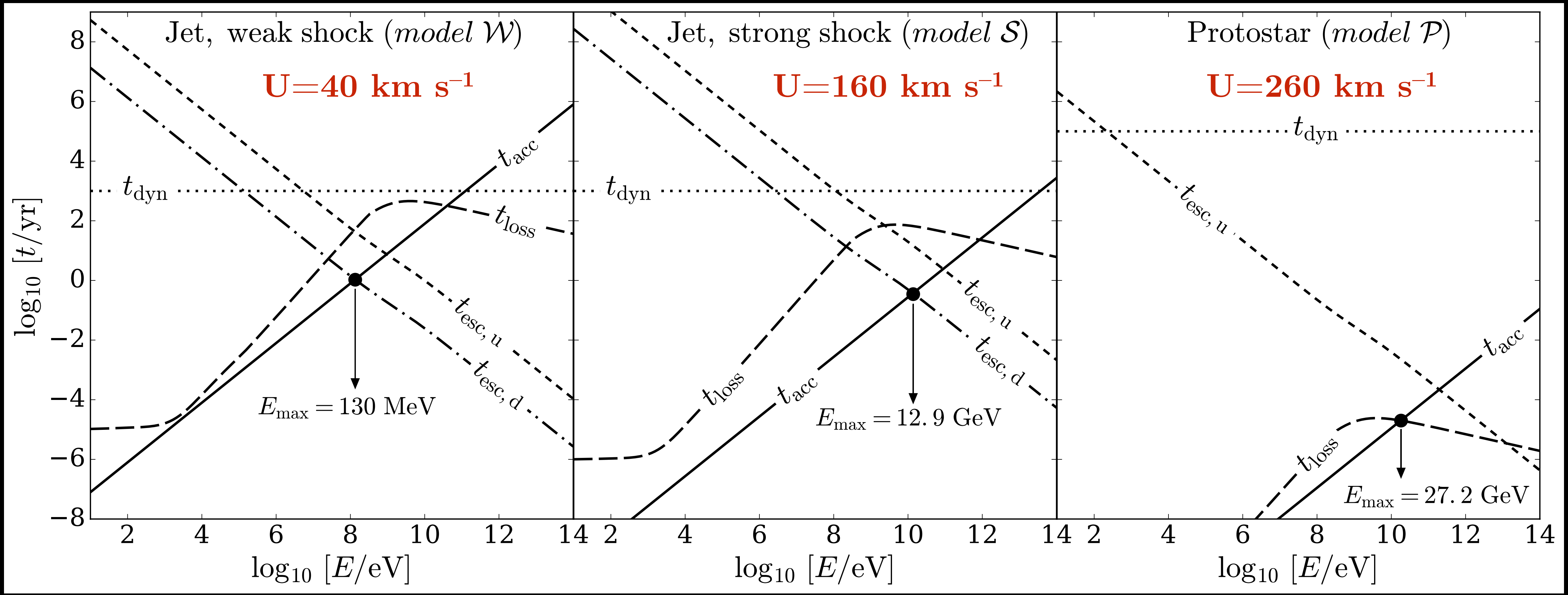

PM, Marcowith, Hennebelle & Ferrière (2017)

The jet morphology is far from being universally defined.

- jet lengths spread over orders of magnitudes;
- usually there is not a single final bow shock, but innermost knots are resolved into bow shocks (time-variable jet emitting dense-gas bullets, McCaughrean+ 2002);
- jet angle variations due to precession (Devine+ 1997) or orbital motions (Noriega-Crespo+ 2011);

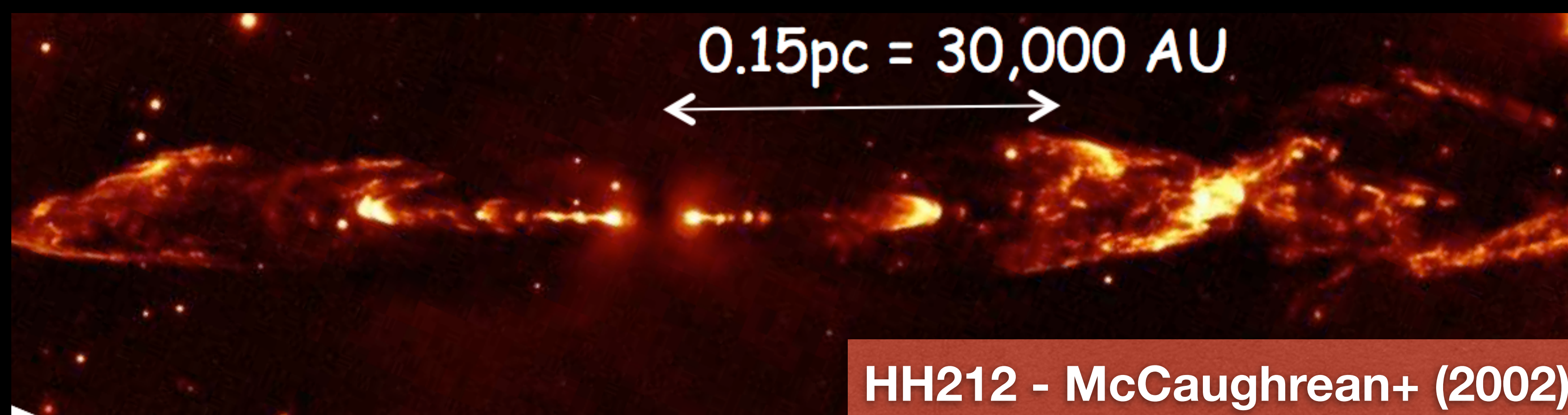

HH212 - McCaughrean+ (2002)

HH111 - Reipurth+ (1999)

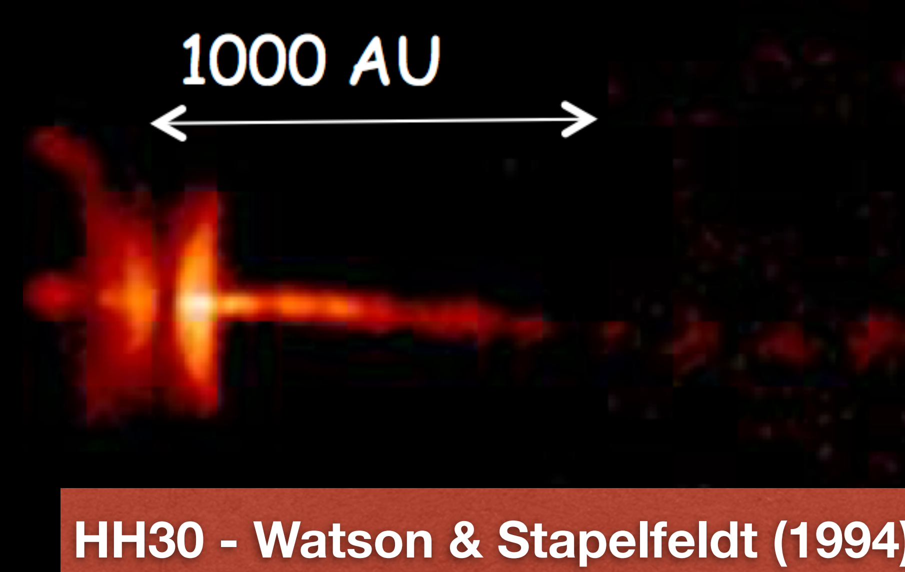

HH30 - Watson & Stapelfeldt (1994)

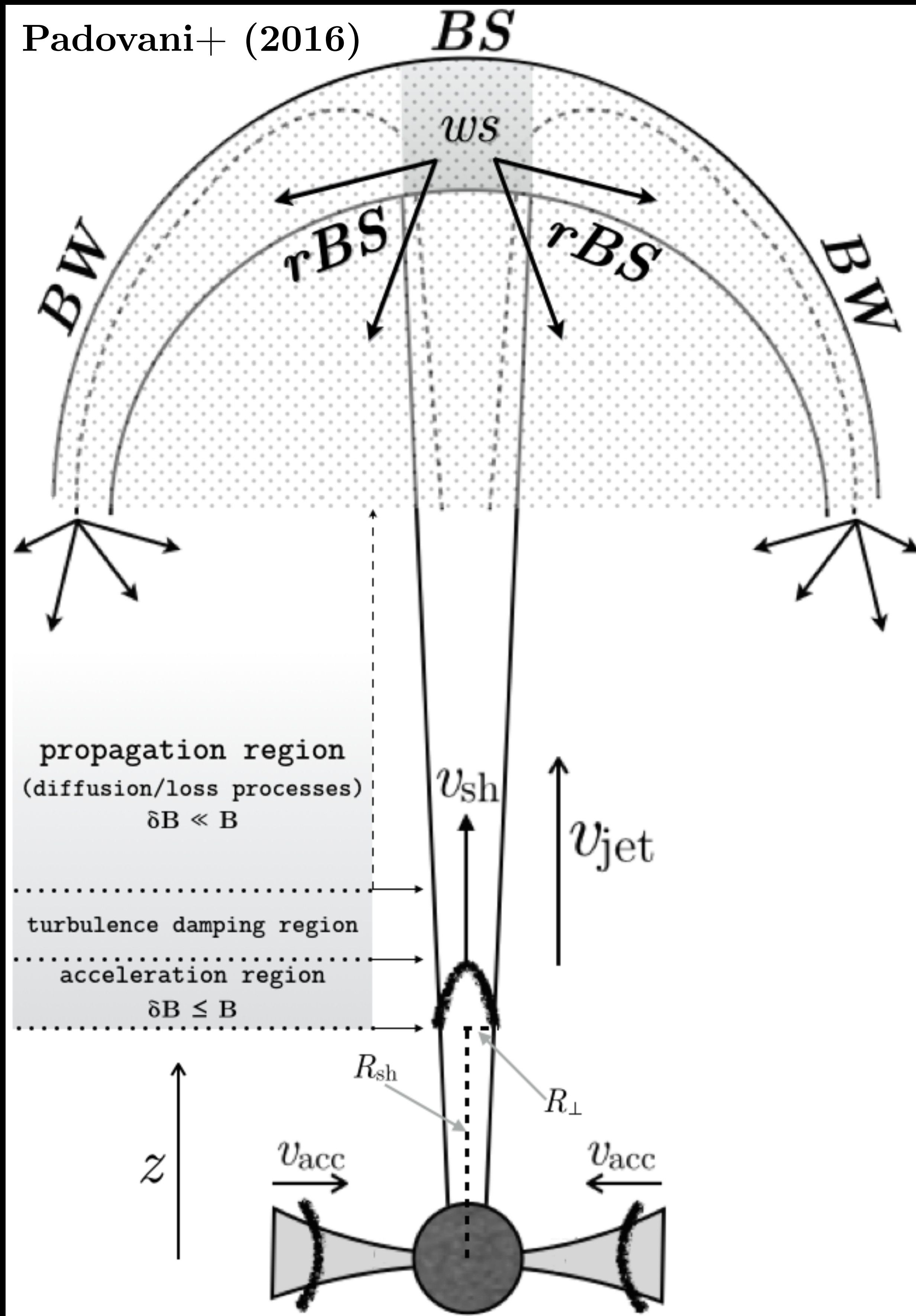

For the sake of clarity we consider

- a single shock at R_{sh}=100 AU from the protostar;
- follow the propagation up to the rBS and the HS.

energy losses (PM, Galli & Glassgold 2009)
magnetic effects (PM & Galli 2011,2013;
PM, Hennebelle & Galli 2013)

Application of the modelling: comparison with available observations

Ainsworth+ (2014) detected synchrotron emission (GMRT) towards the bow shock (knot C) of DG Tau, speculating that this could be due to relativistic electrons accelerated in the interaction between the jet and the ambient medium.

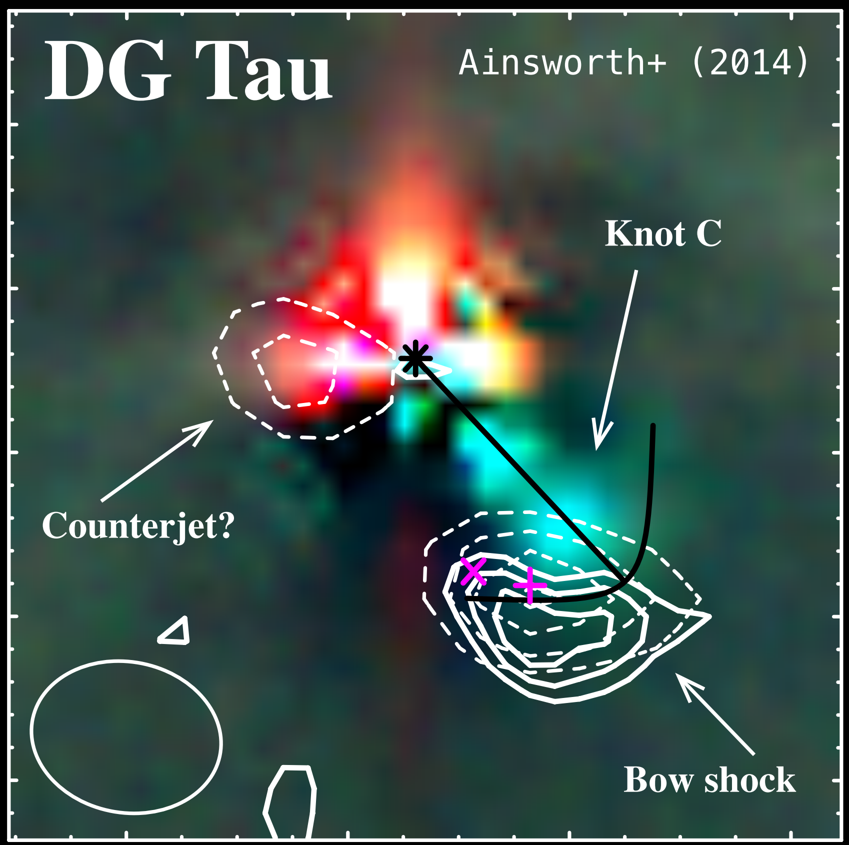

325 MHz (solid contours);
610 MHz (dashed contours).

Using results by Lynch+ (2013), EVLA obs.

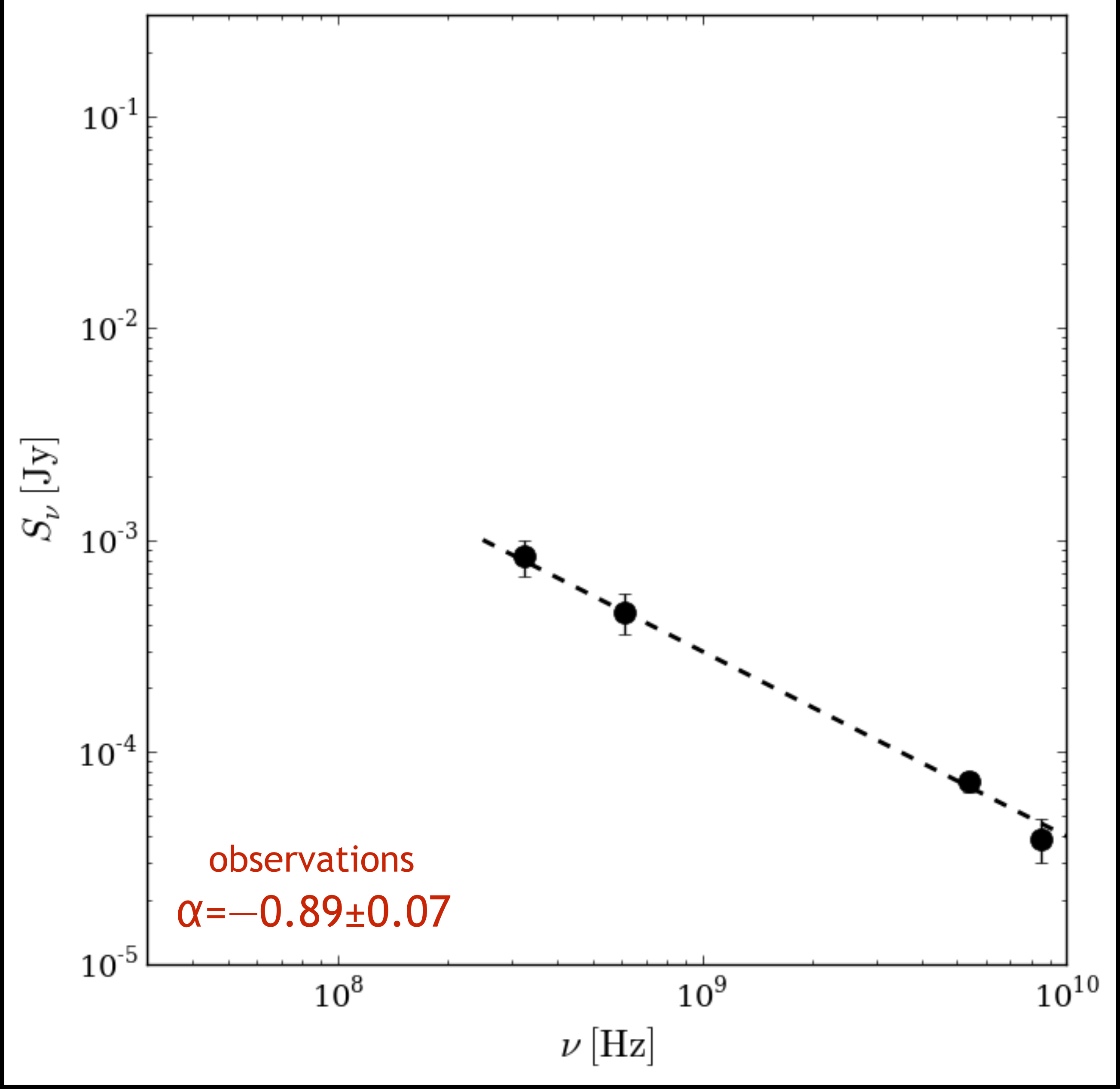

Application of the modelling: comparison with available observations

Ainsworth+ (2014) detected synchrotron emission (GMRT) towards the bow shock (knot C) of DG Tau, speculating that this could be due to relativistic electrons accelerated in the interaction between the jet and the ambient medium.

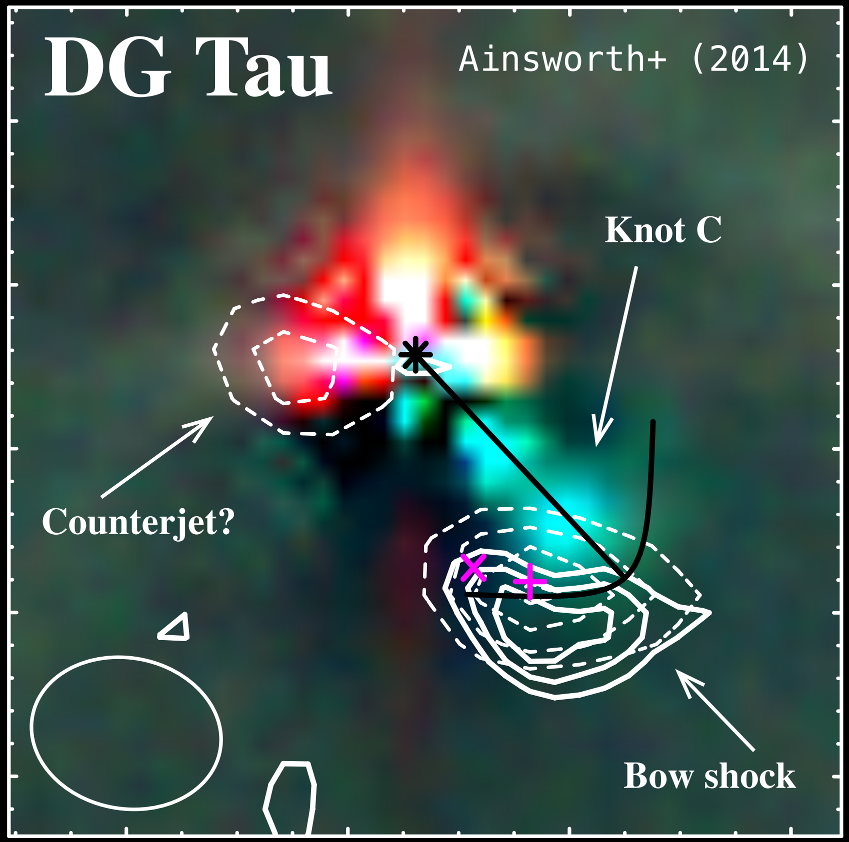

325 MHz (solid contours);
610 MHz (dashed contours).

Using results by Lynch+ (2013), EVLA obs.

- kinematic and physical properties along the jet (McGroarty+ 2009; Oh+ 2015);
- Hypothesis: first acceleration at knot B (Eislöffel & Mundt 1998) plus a re-acceleration at knot C.

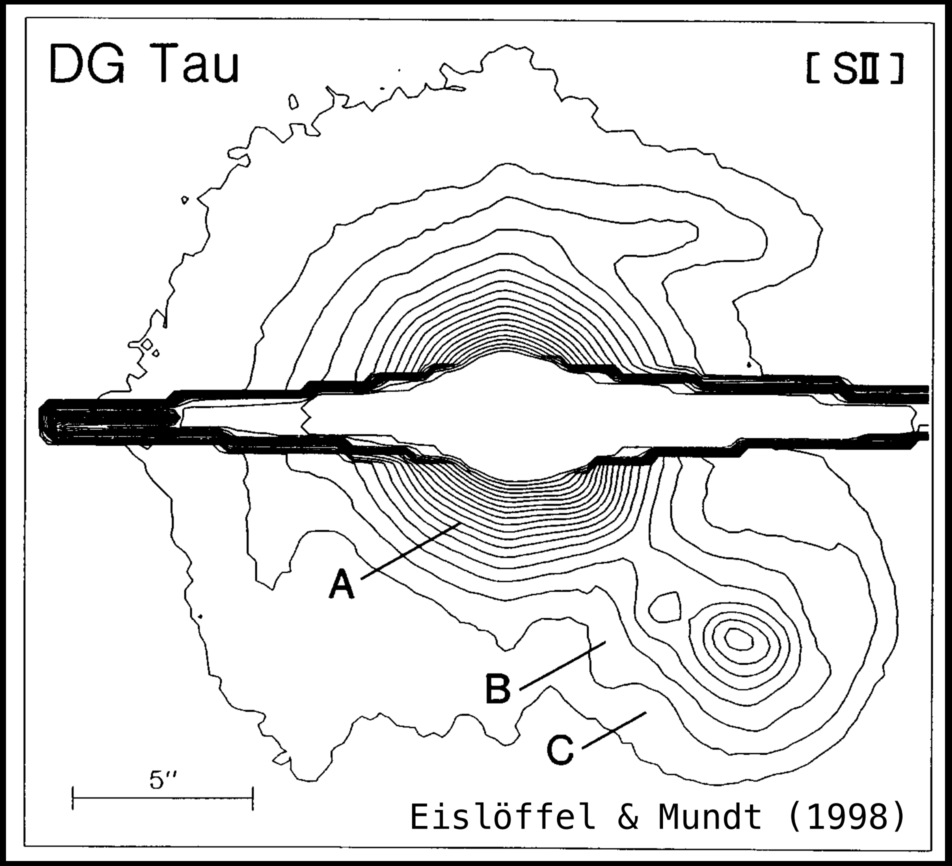

Application of the modelling: comparison with available observations

Ainsworth+ (2014) detected synchrotron emission (GMRT) towards the bow shock (knot C) of DG Tau, speculating that this could be due to relativistic electrons accelerated in the interaction between the jet and the ambient medium.

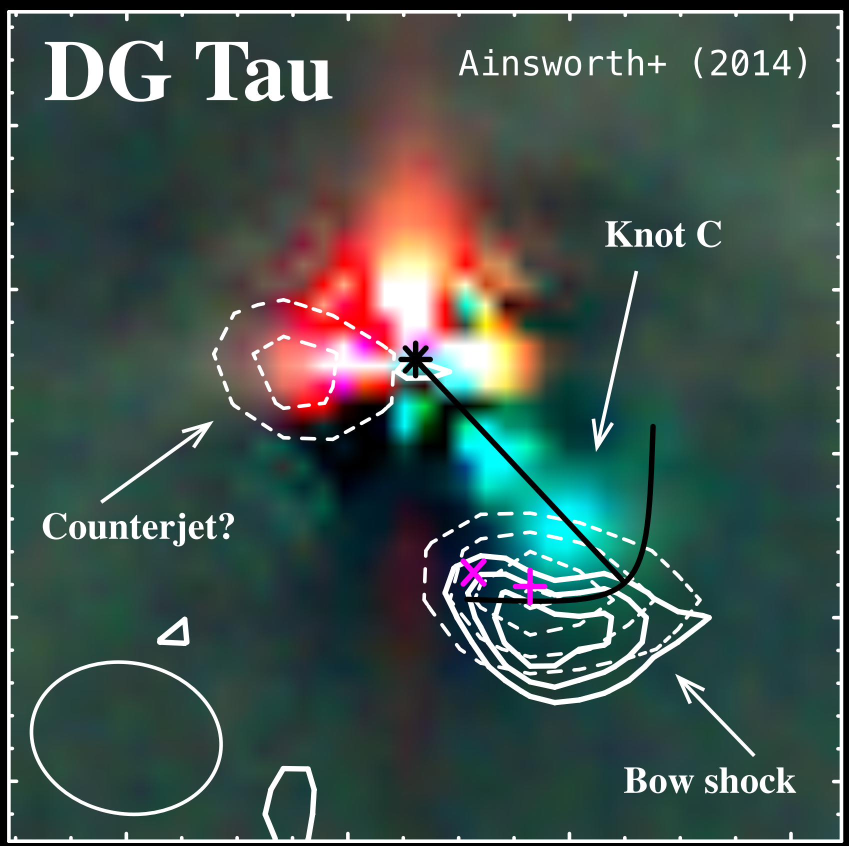

325 MHz (solid contours);
610 MHz (dashed contours).

Using results by Lynch+ (2013), EVLA obs.

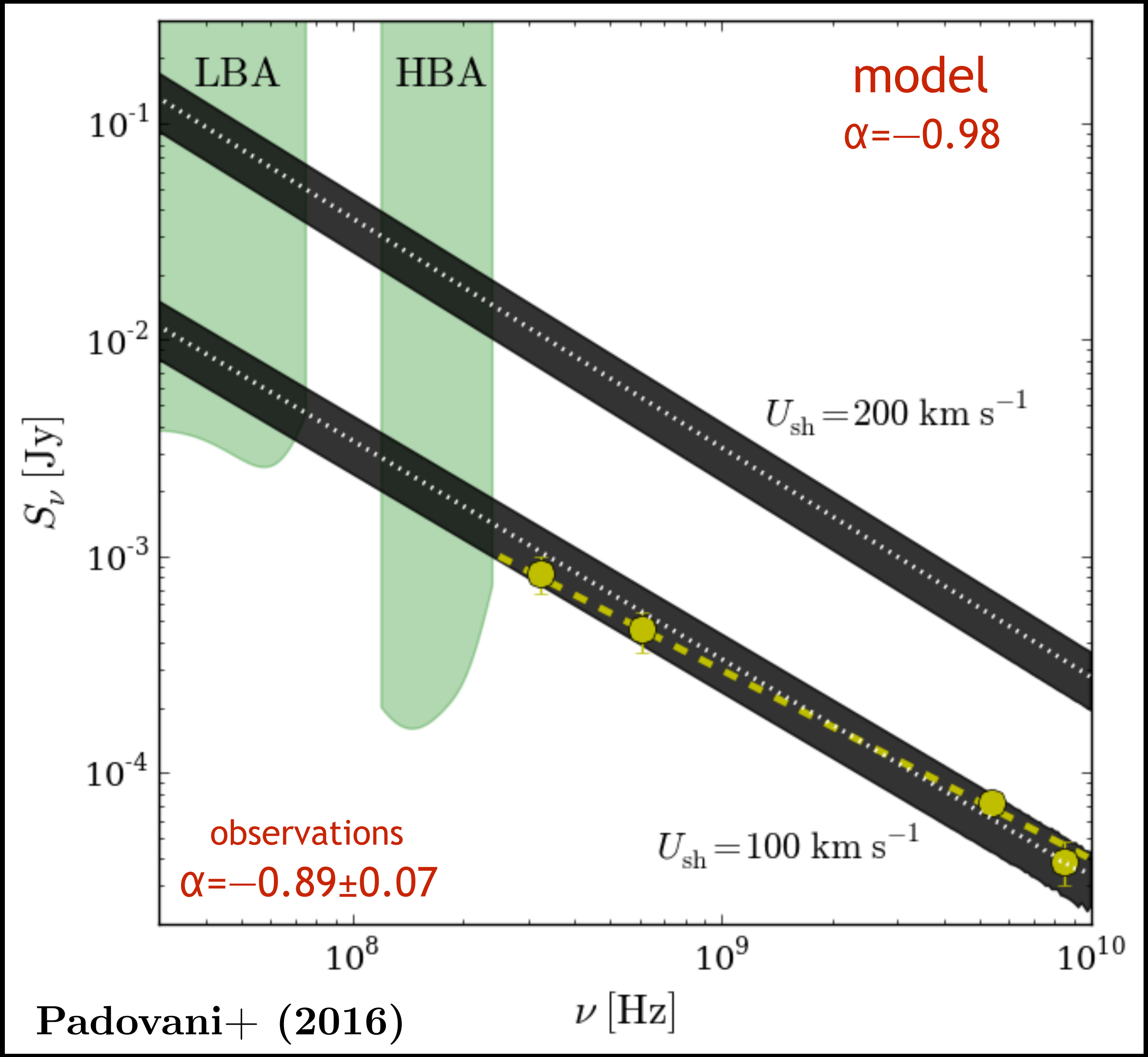

Application of the modelling: comparison with available observations

Ainsworth+ (2014) detected synchrotron emission (GMRT) towards the bow shock (knot C) of DG Tau, speculating that this could be due to relativistic electrons accelerated in the interaction between the jet and the ambient medium.

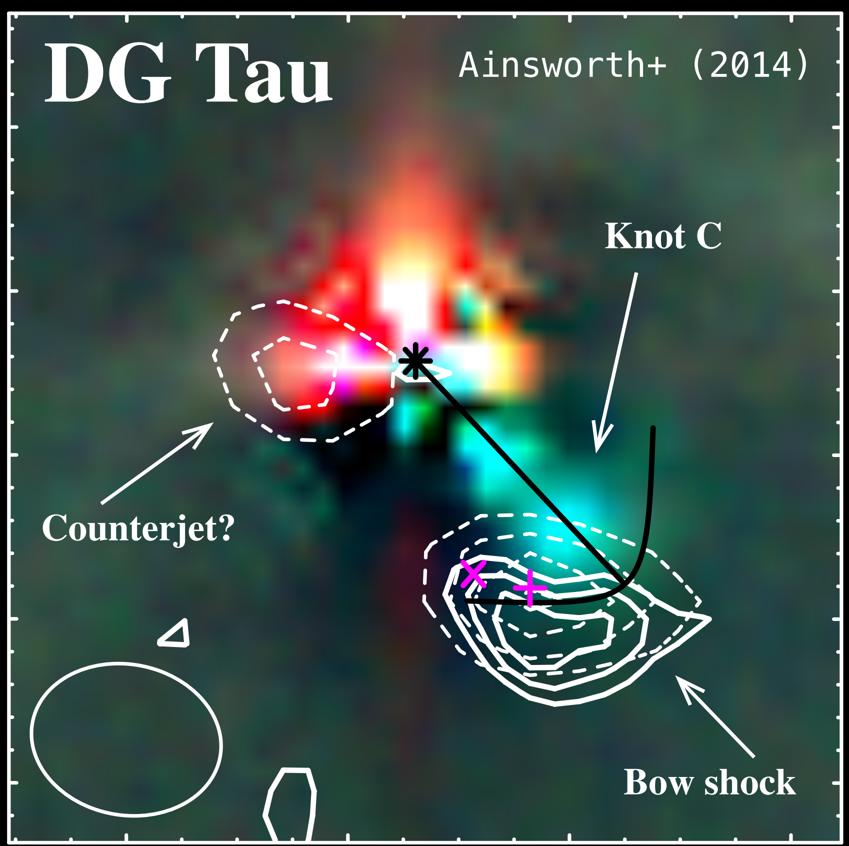

325 MHz (solid contours);
610 MHz (dashed contours).

Using results by Lynch+ (2013), EVLA obs.

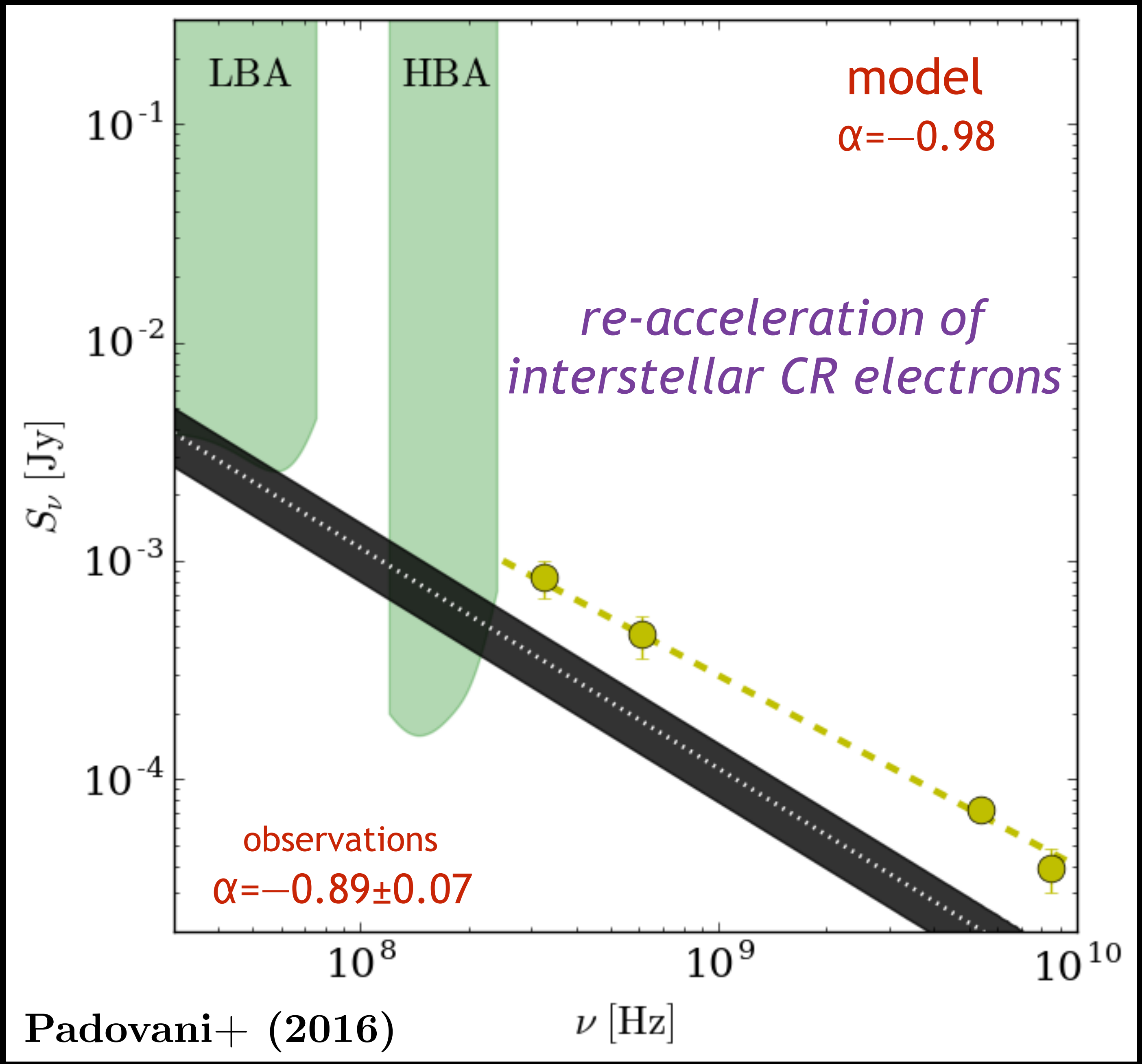

Application of the modelling: comparison with available observations

Podio+ (2014): $\zeta=3\times10^{-16}\ s^{-1}$ in the bow shock B1 in L1157 (HCO^+, N_2H^+).

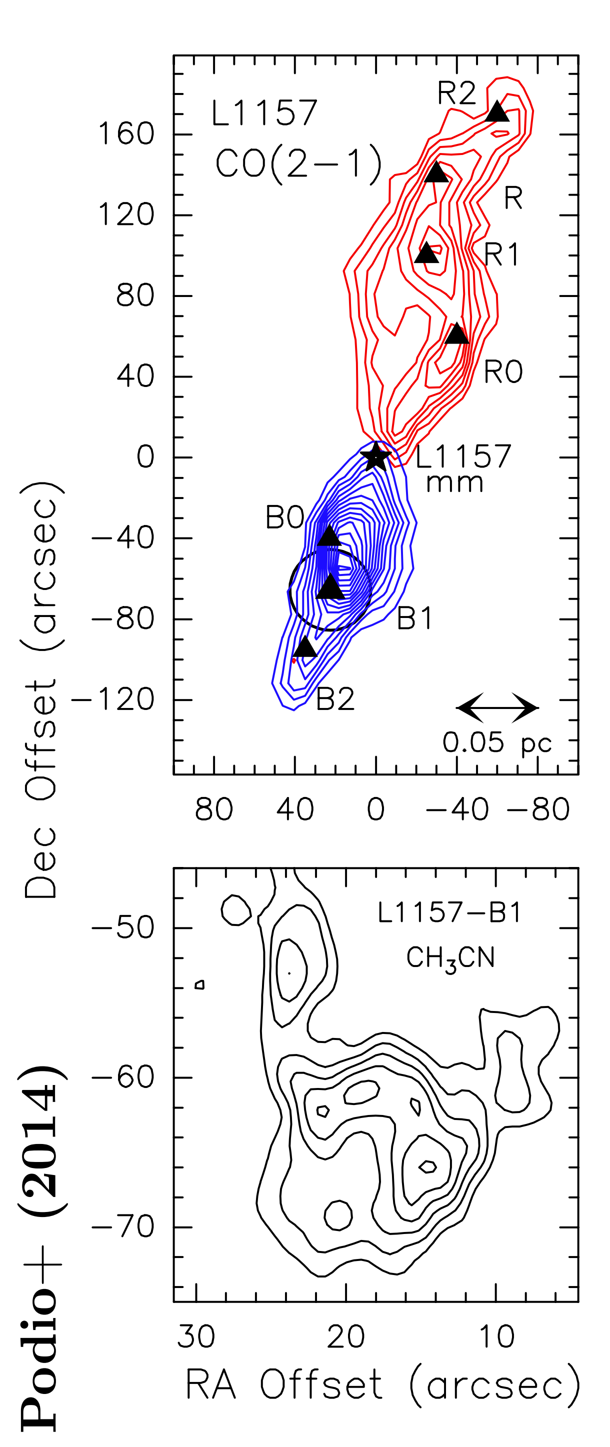

- Youngest knot B0 at 1.2×10^3 AU; B1 at 1.7×10^4 AU with an hot-spot cavity radius of 1.2×10^3 AU (Lefloch+ 2012);
- source distance: 250 pc (Looney+ 2007);
- $v_{flow}\approx100$ km s^{-1}, v_{jet}=20-40 km s^{-1} (Bachiller+ 2001; Tafalla+ 2015);
- $n_H=10^5$-10^6 cm^{-3} (Gómez-Ruiz+ 2015);
- embedded source, T=60-200 K (Podio+ 2014), but hints of T=10^3 K (Busquet+ 2014) to explain water lines.

Our modelling: $\zeta=6.1\times10^{-16}\ s^{-1}$

The values of *all parameters* can vary along the shock surfaces B0 and B1, this is why our result has to be interpreted as a proof of concept.

Need of polarimetric observations (ALMA) to constrain B configuration

Application of the modelling: comparison with available observations

Podio+ (2014): $\zeta=3\times10^{-16}\ s^{-1}$ in the bow shock B1 in L1157 (HCO^+, N_2H^+).

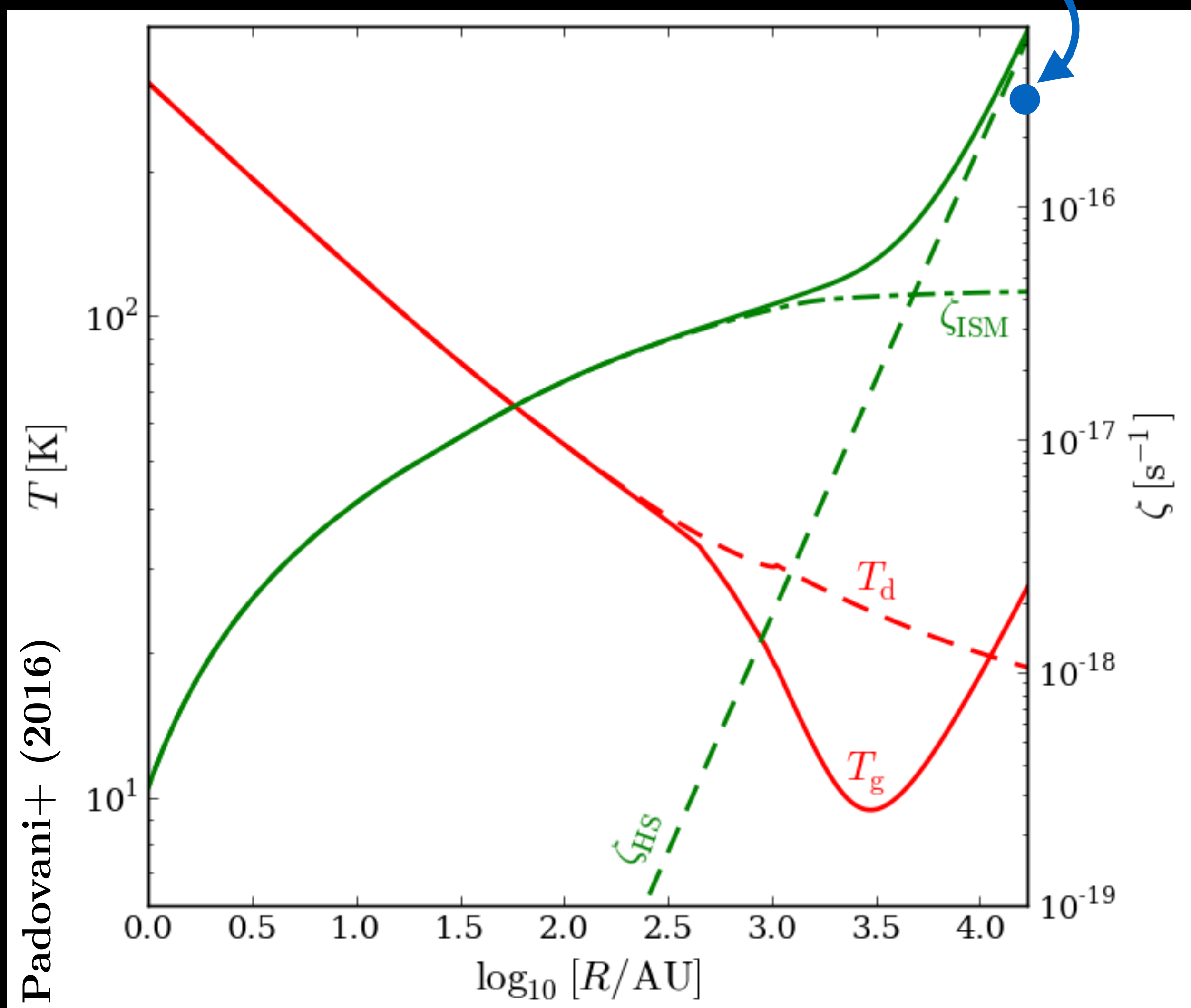

- IS CRs, for a Voyager-like spectrum cannot explain the ionisation rate observed;
- the contribution of the hot spot CR flux become negligible at $R<5\times10^3$ AU (geometric dilution factor).

Check on gas temperature, accounting only for the heating due to IS and locally generated CRs (neglecting UV from ISRF).

$$\frac{T_d(R)}{\mathrm{K}} = 300\left(\frac{R}{\mathrm{AU}}\right)^{-0.41}$$ (Chiang+10,12)

- R<300 AU: gas-dust coupling;
- 300 AU<R<3000 AU: T_g ↓ (IS CR heating weak);
- R>3000 AU: T_g ↑ (hot spot CR heating).

Application of the modelling: comparison with available observations

Ceccarelli+ (2014): $\{\zeta=1.5\times10^{-12}$ s^{-1} at 1600 AU; $\zeta=4\times10^{-14}$ s^{-1} at 3700 AU$\}$ in OMC-2 FIR 4 (HCO^+, N_2H^+).

Protostellar surface acceleration model (parameters from Masunaga & Inutsuka 2000).

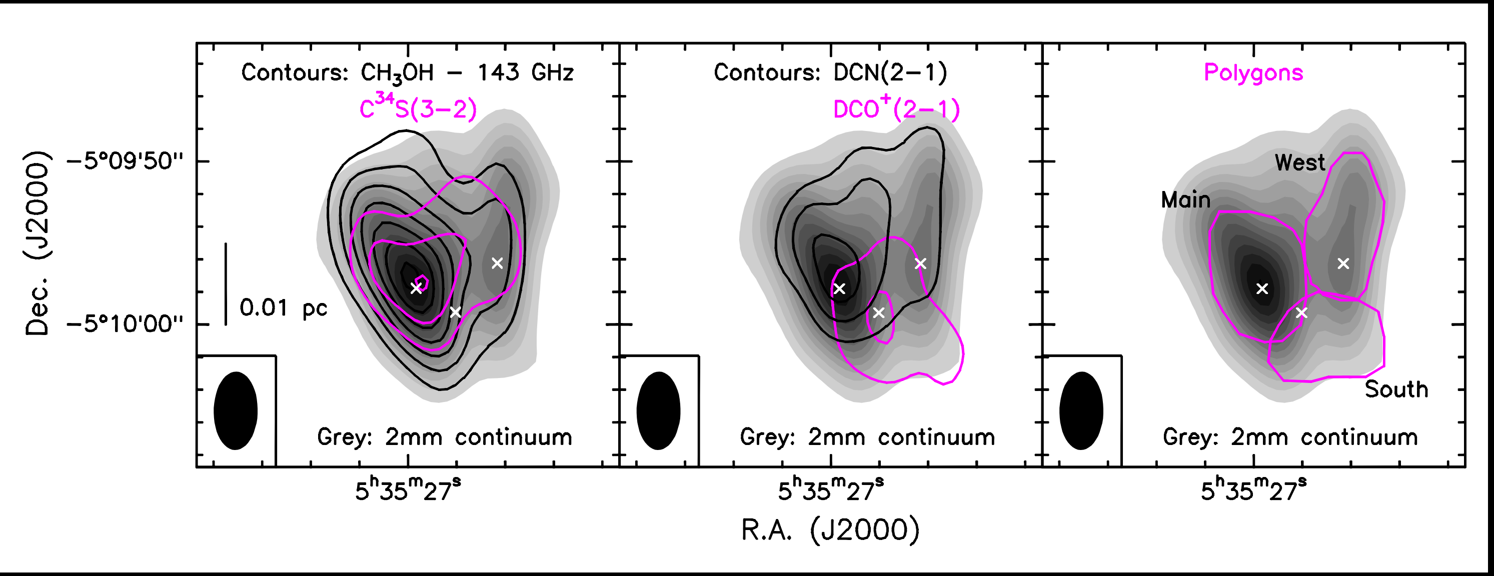

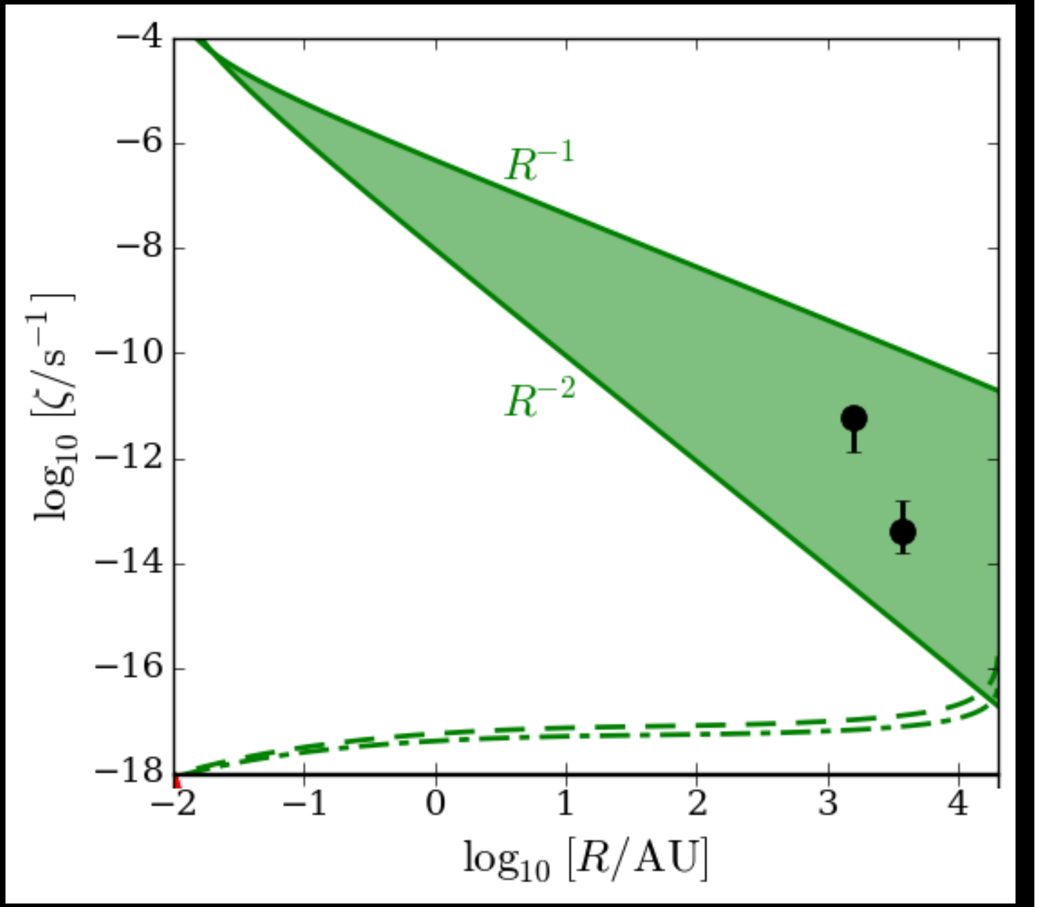

- Geometrical dilution factor:
  - free-streaming case → R^{-2}
  - diffusion with $R_{diff} \gg R$ → R^{-1} (Aharonian 2004)

→ The propagation mechanism is probably neither purely diffusive nor free streaming.

Application of the modelling: comparison with available observations

Local CRs could be responsible for the formation of short-lived radionuclei (^{10}Be) contained in calcium-aluminium-inclusions of carbonaceous meteorites.

$[^{10}\mathrm{Be}]_{\mathrm{meteorites}} \gg [^{10}\mathrm{Be}]_{\mathrm{ISM}}$.

Hypothesis: *spallation reactions* during the earliest phases of the protosolar nebula.

Fluence per unit time: $$\mathcal{F}_t(E_{\min}) = 2\pi \int_{E_{\min}}^{E_{\max}} j(E)\mathrm{d}E$$

$E_{\min} \simeq 50$ MeV: energy threshold for $p +^{16}\mathrm{O} \rightarrow^{10}\mathrm{Be} + \ldots$

$\mathcal{F}_t = 2 \times 10^{17}$ protons cm^{-2} yr^{-1} (purely diffusive case)
$\mathcal{F}_t = 8 \times 10^{18}$ protons cm^{-2} yr^{-1} (free-streaming case)

An irradiation of few tens of years can explain the values of the fluence derived by Gounelle+ (2013) equal to 10^{19}-10^{20} protons cm^{-2}.

Intermittent, cyclic acceleration?

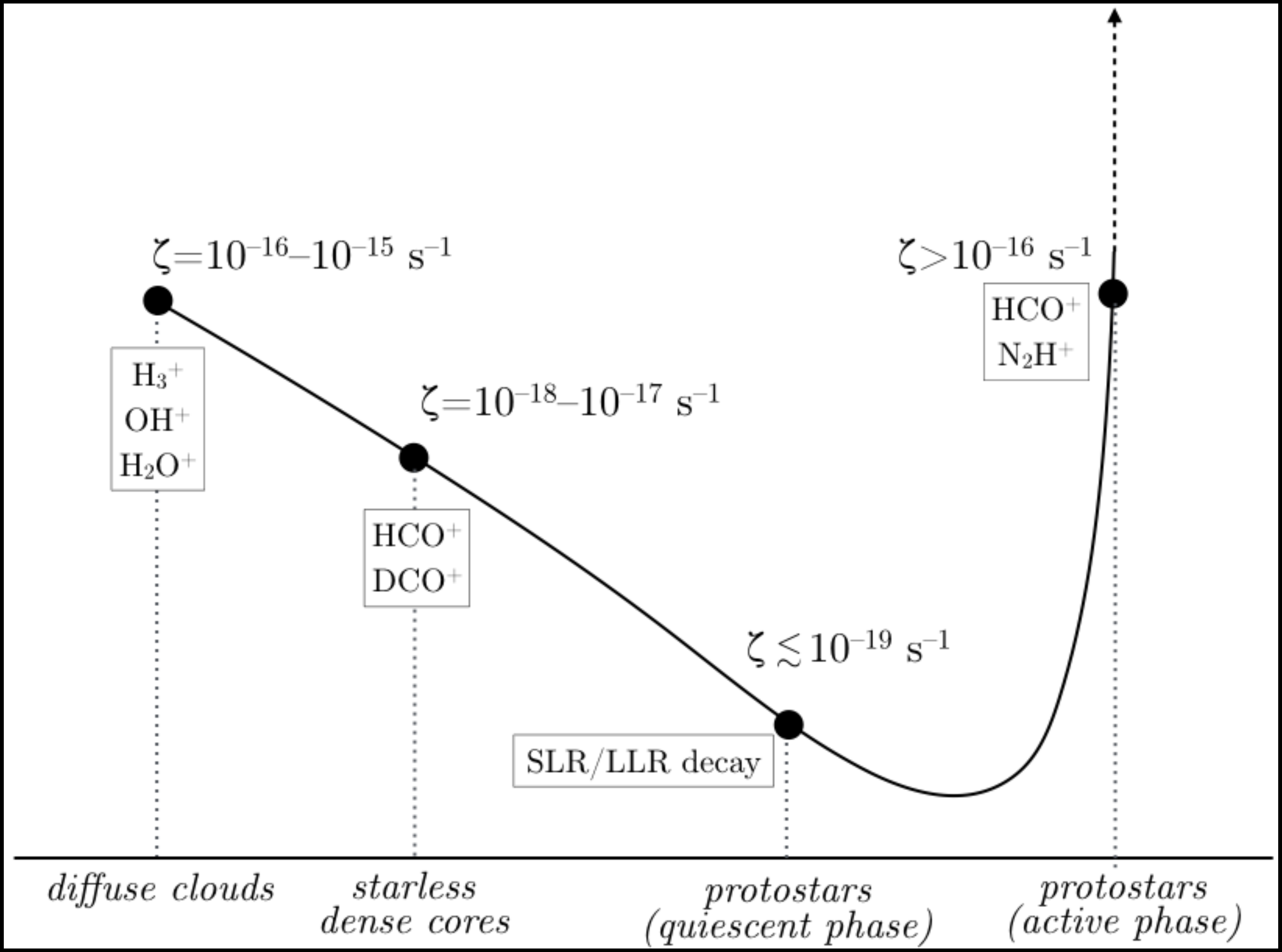

Conclusions and Perspectives

★ Set of conditions to be fulfilled highly non-linear: small variations in one or more parameters (B, x, $n_{\rm H}$, T, $U_{\rm sh}$, η, $k_{\rm u}$) can make the acceleration process inefficient. Since a protostar is a highly dynamic system, particle acceleration can be an intermittent process.

E.g.: a local increase of ζ corresponds to a local variation of x, varying the efficiency of the acceleration mechanism.

★ High-resolution observations (e.g. with ALMA and NOEMA) will help to have better constraints, with a special consideration for the magnetic field configuration. Besides (B, x, $n_{\rm H}$, T, $U_{\rm sh}$, η, $k_{\rm u}$) are not constant all along the shock surface ⇒ modelling improvements.

★ A number of observations can be explained by our modelling: synchrotron emission in DG Tau, ionisation rate in L1157-B1 and OMC-2 FIR 4.

★ The most limiting condition on $E_{\rm max}$ is the geometry of the jet, in particular $R_\perp$. Far from the source, $R_\perp$ increases and less and less particles are lost in the perpendicular directions. Particles can be accelerated up to 1–10 TeV (CTA targets ?).

★ Comparison with possible competing effects (X-ray ionisation).

★ Role of turbulence (Does the dilution factor goes with R^{-2} or R^{-1} ?)

★ We need more observations (statistics).